HHS Public Access

Author manuscript

Comput Chem Eng. Author manuscript; available in PMC 2020 December 05.

Published in final edited form as:

Comput Chem Eng. 2020 December 5; 143: . doi:10.1016/j.compchemeng.2020.107063.

Insights into the interactions of bisphenol and phthalate compounds with unamended and carnitine-amended montmorillonite clays

Asuka A. Orr[a,1], **Shujun He**[a,1], **Meichen Wang**[b,1], **Alicia Goodall**[a], **Sara E. Hearon**[b], **Timothy D. Phillips**[b], **Phanourios Tamamis**[a,c,*]

[a]Artie McFerrin Department of Chemical Engineering, Texas A&M University, College Station, TX, 77843, USA

[b]Veterinary Integrative Biosciences Department, College of Veterinary Medicine and Biomedical Sciences, Texas A&M University, College Station, TX, 77843, USA

[c]Department of Materials Science and Engineering, Texas A&M University, College Station, TX, 77843, USA

Abstract

Montmorillonite clays could be promising sorbents to mitigate toxic compound exposures. Bisphenols A (BPA) and S (BPS) as well as phthalates, dibutyl phthalate (DBP) and di-2-ethylhexyl phthalate (DEHP), are ubiquitous environmental contaminants linked to adverse health effects. Here, we combined computational and experimental methods to investigate the ability of montmorillonite clays to sorb these compounds. Molecular dynamics simulations predicted that parent, unamended, clay has higher binding propensity for BPA and BPS than for DBP and DEHP; carnitine-amended clay improved BPA and BPS binding, through carnitine simultaneously anchoring to the clay through its quaternary ammonium cation and forming hydrogen bonds with BPA and BPS. Experimental isothermal analysis confirmed that carnitine-amended clay has enhanced BPA binding capacity, affinity and enthalpy. Our studies demonstrate how computational and experimental methods, combined, can characterize clay binding and sorption of toxic compounds, paving the way for future investigation of clays to reduce BPA and BPS exposure.

Keywords

Molecular dynamics; Montmorillonite; Bisphenol; Phthalate; Isothermal analysis

[*]Corresponding author: tphillips@cvm.tamu.edu (T.D. Phillips), tamamis@tamu.edu (P. Tamamis).

[1]Equally contributing first authors

Author statement

Asuka A. Orr, Shujun He and Alicia Goodall performed the computational analysis. Meichen Wang and Sara E. Hearon performed the experimental analysis. Asuka A. Orr, Shujun He, Meichen Wang, Timothy D. Phillips and Phanourios Tamamis contributed to the writing of the manuscript. Timothy D. Phillips and Phanourios Tamamis supervised the study.

Declaration of Competing Interest

The authors declare that they have no known competing financial interests or personal relationships that could have appeared to influence the work reported in this paper.

Supplementary materials

Supplementary material associated with this article can be found, in the online version, at doi:10.1016/j.compchemeng.2020.107063.

1. Introduction

Approximately 245 million tons of plastics are produced annually (Halden, 2010). Plastics possess several desirable properties, such as light weight, UV- and chemical-resistance, moldability, insulation, and strength (Andrady and Neal, 2009). Thus, plastics are indispensable in many aspects of life and are integral in several industries including, but not limited to, medicine (North and Halden, 2013), food processing and packaging (Betts, 2011), and electronics (Ramesh et al., 2014). Nevertheless, despite their usefulness, most plastics are not biodegradable (Song et al., 2009) and large amounts of chemicals involved in plastic production, such as bisphenols and phthalates, are released into the environment as a result of urbanization and industrialization (Liaqat, 2018). Bisphenols and phthalates are used in the production of plastics since the development of economical and safe replacements has been difficult (Ritter, 2011; Lioy et al., 2015); thus, they are ubiquitous contaminants in the environment that can affect human health (Centers for Disease Control and Prevention 2018; Teuten et al., 2009).

First synthesized in 1891, bisphenol A (BPA) is a monomeric precursor of polycarbonate plastics (Pjanic, 2017). A significant portion of BPA production has the potential of being in constant contact with food as unbound BPA molecules can leach into food and beverages (Talsness et al., 2009). For example, plastic packaging, reusable food/beverage containers, and kitchenware can leach BPA molecules into food and drinks over time (Talsness et al., 2009; Brotons et al., 1995; Kang et al., 2003; Kubwabo et al., 2009). Furthermore, due to the use of plastics in many other applications, including dental materials and clothing, BPA can be inhaled and transmitted dermally as well (Olea et al., 1996; Wilson et al., 2007). Due to its phenolic structure, BPA is known to interact with estrogen receptors and thereby has been linked to endocrine disorders including male infertility, precocious puberty, breast and prostate cancer, and several metabolic disorders (Tarapore et al., 2014; Konieczna et al., 2015). In addition to its adverse effects related to its estrogenic activity, epidemiologic evidence also implicates BPA in cardiovascular disease, type 2 diabetes mellitus, and obesity (Konieczna et al., 2015; Lang et al., 2008; Shankar and Teppala, 2011; Wang et al., 2012).

Due to the health concerns revolving around BPA, bisphenol S (BPS) was initially introduced as a possible safer alternative to BPA. However, due to its structural similarity to BPA, BPS was also suggested to be an endocrine disruptor (Moon, 2019). In human adrenocortical carcinoma cell line, BPS was shown to affect the synthesis of various hormones such as cortisol testosterone and progesterone (Feng et al., 2016; Rosenmai et al., 2014). Additionally, BPS has weak estrogenic activity in *D.magna* as shown by *in vivo* studies (Chen et al., 2002), can reduce plasma and intra-testicular concentrations of testosterone as well as induce oxidative stress in rats (Ullah et al., 2016; Ullah et al., 2019), and can influence female mammary gland development in mice (Kolla et al., 2018). BPS can also lead to severe reproductive defects, as shown by studies with *C. elegans* where exposure to BPS led to increased embryonic lethality and decreased brood size (Chen et al., 2016) as well as impaired non-associative learning in adults after exposure during early embryogenesis (Mersha et al., 2015). Analogous to BPA, BPS can still leach from household products, albeit to a lesser degree compared to BPA (Viñas et al., 2010; Russo et al., 2018).

Additionally, compared to BPA, BPS has a longer half-life and is less biodegradable, leading to more persistent accumulation in the environment (Héliès-Toussaint et al., 2014).

Apart from BPA and BPS, phthalates are also indispensable in the production of plastics. Phthalates including dibutyl phthalate (DBP) and di-2-ethylhexyl phthalate (DEHP) are plasticizers capable of increasing flexibility, pliability, and elasticity of otherwise rigid polymers (Chou and Wright, 2006). They are heavily used in industry to produce products such as household items, paints, and medical devices. Phthalate networks are not covalently connected, allowing them to leach into the environment and subsequently in the human body (Braun et al., 2013; Mihucz and Záray, 2016; Bošnir et al., 2007). As a result, exposures of phthalates are a global problem that can pose a threat to human health (Jensen et al., 2012; Swan et al., 2005). DBP was suggested to be an endocrine-disruptive chemical and toxic to various organisms (Clewell et al., 2010; Hu et al., 2009; Ortiz-Zarragoitia et al., 2006; Xu et al., 2013). Animal studies on DBP have shown that it causes oxidative damage in rat kidney and inhibitory effects on the SOD (Superoxide dismutase) enzyme by occupying the SOD-active site (Prasanth et al., 2009). Human studies also showed that DBP could have adverse effects on the male reproductive system (Chang et al., 2015; Bloom et al., 2015). DEHP was also suggested to be an endocrine-disruptive chemical (Grindler et al., 2018). Rodent experiments revealed that exposure to DEHP can lead to reproductive anomalies, adverse liver effects, and even cancer (Gray et al., 2009; Rusyn et al., 2006). Furthermore, DEHP can lead to increased proliferative activity of Leydig cells in rats treated with DEHP and induction of Leydig cell hyperplasia (Akingbemi et al., 2004).

BPA, BPS, DBP and DEHP are environmental contaminants, which among others, are potent endocrine disruptors that can negatively affect human and animal reproductive systems. Thus, effective strategies that can mitigate their toxicities in humans and animals are critically needed. Extensive work in the literature focuses on removal of chemical contaminants from water using electrochemical reaction (Boscolo Boscoletto et al., 1994; Gözmen et al., 2003), filtration (Liu et al., 2009; Asada et al., 2004; Nakanishi et al., 2002; Tsai et al., 2006; Wirasnita et al., 2018; López-Ramón et al., 2019; Toor and Mohseni, 2007; Mohan et al., 2007), photo-Fenton process (He et al., 2009; Kovačič et al., 2019; Chen et al., 2009; Zhang et al., 2019), and membrane process (Bodzeka et al., 2004).

Montmorillonite clays have been extensively studied and reported to tightly bind various chemicals within their interlayers, including aflatoxins and certain pesticides (Jaynes and Boyd, 1991; Sposito et al., 1999; Hearon et al., 2020; Aristilde et al., 2010). Previous intervention studies and clinical trials have shown that mineral adsorbents, including montmorillonite clays, significantly decrease biomarkers of aflatoxin exposure and could be safely consumed by humans and animals on a short-term basis (Phillips et al., 2019; Colvin et al., 1989; Phillips et al., 1990; Phillips et al., 1991; Phillips et al., 1994; Phillips et al., 1995; Kubena et al., 1990; Kubena et al., 1991; Kubena et al., 1993; Bonna et al., 1991; Harvey et al., 1994; Harvey et al., 1991a; Harvey et al., 1991b; Jayaprakash et al., 1992; Lindemann et al., 1993; Mitchell et al., 2014; Pollock et al., 2016; Awuor et al., 2017; Maki et al., 2017; Wang et al., 2019). Moreover, montmorillonite clays that have been amended with natural nutrients, such as carnitine, are broad-acting and have shown increased effectiveness in their ability to bind diverse hazardous organic compounds and toxic metals

(Wang et al., 2017; Wang et al., 2019; Li and Wu, 2010; Cruz-Guzmán et al., 2004). Thus, we aimed to explore whether montmorillonite clays bind to endocrine disrupting contaminants such as BPA, BPS, DBP, and DEHP, and additionally whether carnitine-amended montmorillonite clays could further enhance the binding to the compounds.

The major objective of this study was to evaluate binding and sorption properties and the mechanisms for the potential sorption of BPA, BPS, DBP, and DEHP onto surfaces of montmorillonite clay and carnitine-amended montmorillonite clay using molecular dynamics (MD) simulations and experimental isothermal analyses. MD simulations can provide fundamental insights into binding mechanisms between montmorillonite clay with the investigated plastic monomers and plasticizers. Previous computational studies have successfully characterized stable configurations and associated potential energies of organic compounds on clay surfaces for various organic compounds using MD simulations (Aristilde et al., 2010; Wang et al., 2019; Aggarwal et al., 2007; Kristof et al., 2018; Willemsen et al., 2019; Samaraweera et al., 2014).

In this study, we performed a detailed evaluation of the binding of BPA, BPS, DBP, and DEHP to montmorillonite clays using structural analysis and energetic calculations on the simulation snapshots produced. Specifically, multiple simulations followed by subsequent structural and energetic calculations of 8 systems comprising a modeled montmorillonite clay (unamended clay) or carnitine-amended montmorillonite clay (amended clay) in the presence of the multiple copies of the 4 compounds, independently, were conducted to determine: (1) binding propensity and binding persistence of BPA, BPS, DBP, and DEHP for clay; (2) binding sites on active surfaces within the clay interlayer and the basal surface of the clay; (3) interaction energies; (4) binding modes. Importantly, the results derived from computational MD simulations were compared with *in vitro* experimental results from adsorption isotherms, including binding capacity, binding affinity, and thermodynamics of sorption (free energy and enthalpy).

2. Methods

2.1. Simulations setup

We performed quintet 100 ns simulations of different simulation systems modeling unamended montmorillonite clay and carnitine-amended montmorillonite clay in the presence of multiple copies of BPA, BPS, DBP, and DEHP compounds, independently. Each of the investigated simulation systems was built and simulated using methods analogous to our previous study (Wang et al., 2019). We used the two-layered montmorillonite clay model reported in our previous study (Wang et al., 2019) as our initial structure of the clay with a stoichiometry of $(Si_4)^{IV}(Al_{1.67}Mg_{0.33})^{VI}O_{10}(OH)_2$. This model was generated by periodically replicating a 2.5 × 2.5 nm^2 montmorillonite clay layer extracted from the INTERFACE MD model database (Heinz et al., 2013; Heinz et al., 2005) to build a single 5 × 5 nm^2 layer. The single 5 × 5 nm^2 clay layer was then replicated to build a second 5 × 5 nm^2 clay layer with a d_{001} spacing of 21 Å from the first clay layer (Wang et al., 2019; Wang et al., 2017). The two-layered montmorillonite clay model was solvated in a 90 × 90 × 90 $Å^3$ acetonitrile box (Wang et al., 2019).

For the simulations of the unamended clay in the presence of BPA, BPS, DBP, and DEHP, independently, 24 toxic compounds were initially dispersed around the clay within the 90 × 90 × 90 $Å^3$ acetonitrile box in random configurations and orientations. For the simulations of the carnitine-amended clay, hereinafter referred to as the amended clay, in the presence of the toxic compounds, the modeled clay was first equilibrated in the presence of carnitine prior to the introduction of toxic compounds to derive the initial structure of the amended clay. The introduction of carnitine to unamended clay to model the amended clay prior to the introduction of any toxic compounds was performed to mimic experimental conditions. Experimentally, the amended clay was formed by mixing the unamended clay with carnitine in solution and subsequently centrifuging and washing the resulting amended clay with distilled water. Thus, initially in the simulations, 24 carnitine molecules were dispersed around the clay in random configurations and orientations. After a short 10 ns simulation, representing the initial mixing of the unamended clay with carnitine in experiments, the coordinates of the clay and 12 individual carnitine compounds bound to the clay were extracted and used as the initial structure of the amended clay, aiming to represent the washed amended clay in experiments. The remaining 12 carnitine compounds were not included as they were not bound to the clay in the 10 ns snapshot. Subsequently, the 24 toxic compounds were placed in the vicinity of the amended clay with the same positions, orientations, and configurations as used for the unamended clay.

For both the simulations of the unamended clay and the amended clay, the initial random configurations of both the toxic compounds and carnitine were generated from short 1 ns simulations of single compounds at infinite dilution using the generalized Born with a simple switching implicit solvent model (Im et al., 2003) with the initial molecular structures extracted from the ZINC database (Sterling and Irwin, 2015). The concentration of toxic compounds within the simulations corresponded to 0.055 M, which was larger than that used in the experimental studies, aiming to enhance the statistical sampling and accelerate the potential sorption of toxic compounds to the clay surfaces within the simulations similarly to our previous studies (Wang et al., 2019; Tamamis et al., 2009; Chen et al., 2020; Tao et al., 2020). Additional preliminary duplicate MD simulations of the unamended clay in the presence of benzene, which according to experiments minimally binds to montmorillonite clay, at high concentrations showed that benzene only forms sporadic interactions with the clay surface and has a binding percentage of less than 0.05% in the simulations. Thus, while the higher concentration of toxic compounds within the simulations could potentially lead to an overestimation of binding capacity for a given compound, it is not expected to show high binding capacity for a compound that minimally binds to the clay, and the simulations appear to have the capacity to sufficiently screen which toxic compounds can sorb onto the clay. Therefore, the reported statistics aim to provide a primarily qualitative comparison of the toxic compounds' binding for the clays rather than quantitative binding capacities.

Following an analogous methodology to our previous study (Wang et al., 2019), prior to each 100 ns MD simulation run, each simulation system was initially energetically minimized and equilibrated. The energetic minimizations were executed through 500 steps of steepest gradient descent minimization, 500 steps of Newton-Rapson minimization, and 500 steps of steepest descent minimization followed by a constrained 1 ns MD simulation

equilibration stage. Throughout the energy minimizations and 1 ns equilibration stage, the montmorillonite layers and the compounds were constrained with a 1 kcal mol^{-1} $Å^{-1}$ harmonic constraint on all heavy atoms. Following energy minimization and equilibration, all constrains on the simulation system were released except for light 0.1 kcal mol^{-1} $Å^{-1}$ harmonic constraints on aluminum atoms of the clay layers and the systems were simulated for 100 ns with a temperature of 300 K and a pressure of 1 atm. Periodic boundary conditions were applied in the MD simulations. Hydrogen bond lengths were constrained using the SHAKE algorithm. MD simulation snapshots were extracted in 20 ps intervals for subsequent analysis. Five 100-ns replicates of MD simulations with different initial velocities were performed for each system for an aggregate simulation time of 500 ns. All MD simulations and setup were conducted in CHARMM (Brooks et al., 2009) using CHARMM v39b2.

Parameters and topologies used in the simulations for the montmorillonite clay layers were extracted from the INTERFACE force field (Heinz et al., 2013; Heinz et al., 2005). The INTERFACE force field can operate as an extension of commonly used harmonic force fields, e.g. CHARMM, and therefore enables simulation of systems that contain a combination of organic/biomolecular and inorganic interfaces (Pacella and Gray, 2018; Emami et al., 2014; Heinz et al., 2006; Mako et al., 2014) as well as montmorillonite (Wang et al., 2019; Heinz et al., 2005). All studied compounds were parameterized using CGENFF (Vanommeslaeghe et al., 2010; Vanommeslaeghe and MacKerell, 2012; Vanommeslaeghe et al., 2012) with low penalties. The CHARMM36 and the CHARMM general force field was used to model the acetonitrile solvent and counter ions (Vanommeslaeghe et al., 2010; Huang and MacKerell, 2013).

2.2. Analysis procedure

Upon completion of the quintet MD simulations of the unamended or amended clays in the presence of the four compounds, independently, the extracted simulation snapshots were analyzed using in-house programs to study binding propensities and key mechanisms of toxic compound binding to clay (Wang et al., 2019). The first 20 ns of each 100 ns simulation were considered to be equilibration in accordance with the convergence of binding percentage, and the last 80 ns of each simulation were analyzed. Thus, in what follows, the statistical analysis was performed over the last 80 ns in all cases. All structural analyses were performed using in house developed Python programs and all energy calculations were performed using CHARMM (Brooks et al., 2009). The analysis programs were written in Python using the MDAnalysis (Michaud-Agrawal et al., 2011) Python library. An overview of the analysis procedure is presented in Fig. 1.

2.2.1. Propensities of toxic compounds binding to unamended and amended clays

2.2.1.1. Overall binding percentages: To quantitatively evaluate the propensities of compounds (toxic and amending compounds) binding to the clay, we calculated their binding percentage to the unamended and amended clays within their respective simulations. Specifically, the binding percentages were calculated as the cumulative number of instances in which a compound was bound to the clay (binding instances) divided by the product of

the total number of analyzed snapshots and the total number of compounds in the simulation system.

For the unamended clay and amended clay, a toxic compound was defined to be binding directly to the clay (self-binding) based on orthogonal distance cutoffs to the clay layers. The clay layers were represented as planes defined by the aluminum atoms at the center of each clay layer. In addition, because each clay layer was square, two side planes per clay layer perpendicular to the plane representing the clay layer were used to evaluate horizontal proximity. A toxic or amending compound was considered to be binding to a clay layer whenever any of the non-hydrogen atoms have an orthogonal distance within 6.5 Å to the plane representing the clay layer (equivalent to 3.5 Å to the clay surface) and met the side plane cutoffs. Side plane cutoffs dictate that any compound has to be either in the square cylinder of the clay layers or within 3.5 Å to the exterior of the clay. The distance cutoffs, along with visualization of self-binding are illustrated in Fig. 2.

For the amended clay, an amending compound was considered to be binding to the clay using the same aforementioned criteria defining self-binding. Our analysis showed that the binding percentage of carnitine to the clay in all simulations of the amended clay was 70%, confirming and in line with previous experiments showing that carnitine can act as an amending compound to form carnitine-amended clay (Wang et al., 2017; Cruz-Guzmán et al., 2004; Wang et al., 2019). Additionally, a toxic compound was defined to be binding indirectly to the clay (assisted-binding) if the compound was interacting with an amending compound (carnitine), which was simultaneously bound to the clay. The compound was considered to be interacting with an amending compound if any of its atoms were within 3.5 Å of the amending compound. Visualization of assisted-binding is illustrated in Fig. 2.

Two categories of binding were considered in the calculations: self-binding, for which a compound was bound directly to the clay, and assisted-binding, for which a compound was bound indirectly to the clay through an amending compound (carnitine). For the case of unamended clay, only self-binding was possible as no amending compounds were present; for the case of an amended clay, both self-binding and assisted-binding were possible: If a toxic compound was binding to the clay and not within 3.5 Å of any amending compound, the toxic compound was considered to be self-binding; otherwise, if any of a toxic compound’s atoms were within 3.5 Å of a bound amending compound, the toxic compound was considered to be assisted-binding (Fig. 2). Thus, for the systems of unamended clay in the presence of the toxic compounds, self-binding percentages were calculated only, while for systems of amended clay in the presence of toxic compounds, both self-binding and assisted-binding percentages were calculated.

2.2.1.2. Additional insights into the overall binding propensities: To obtain additional insights into the binding propensities and the driving forces leading to the toxic compounds binding to unamended or amended clays, we calculated the electrostatic and van der Waals interaction energy of the toxic compounds binding to the clays. For the cases in which the toxic compound participates in self-binding to either the unamended or amended clay, the interaction energies were calculated directly between the bound toxic compound and the clay. For the cases in which the toxic compound participates in assisted-binding to the

amended clay, the interaction energies were calculated between the bound toxic compound and the amended clay, where only the carnitine compound involved in assisted-binding was included as part of the amended clay. All energy calculations were performed in CHARMM (Brooks et al., 2009) using infinite cutoffs. Importantly, the interaction energy values showed the strength of interaction between the bound toxic compound and the clay, and do not represent the absolute binding affinity of the toxic compounds for the clay.

To evaluate the persistence (stability) of binding by the toxic compounds to the clay, we calculated the residence times of the toxic compounds binding to the clay. First, a binding event was defined as a series of two or more consecutive snapshots where a compound was binding to the clay. A grace period of 20 ps (one snapshot) was introduced so that spontaneous loss of contact does not interrupt a binding event. Residence times were then calculated as the average duration of binding events (i.e. cumulative time of all binding events divided by the total number of binding events). For the simulations of the amended clay, residence times were decomposed into self-binding and assisted-binding residence times. It is important to note that our definition of residence time is microscopic and can be an underestimation of the total macroscopic residence time of compounds binding to the clay, since a loss of contact for even up to tens of nanoseconds may not be significant macroscopically but will significantly decrease the residence time by our definition; in addition, the size of the actual clay interior surface is significantly larger in comparison to its size in simulations, which could be another reason for the possible underestimation of residence in the simulations.

Another important characteristic of the clay was that the properties of the interior and exterior (surfaces) of the clay differ in their binding properties. Therefore, to examine the different binding properties of the compounds between these two types of surfaces, we additionally distinguished based on the interior versus the exterior of the clay. A toxic compound was considered to be binding within the interior of the clay if at least half of the compound's atoms were within the square cylinder formed by 2 clay layers. Otherwise, the toxic compound was considered to be binding to the exterior of the clay. We calculated the percentage of the toxic compounds binding to the interior of the clay (interior percentage) in the case that the toxic compounds were self-binding to unamended clay as well as self-binding and assisted-binding to amended clay. Furthermore, to determine the solvent exposure of specific clay atoms, we calculated the solvent accessible surface area (SASA) of the clay. SASA's of interior and exterior oxygen atoms of the clay layer were averaged across all snapshots of all simulated systems. Because acetonitrile was used as the solvent in our system, SASA calculations were performed with a probe radius of 2.2 Å, instead of 1.4 Å, which is commonly used for water.

2.2.2. Derivation of most populated binding modes within simulations and correlation between structural and energetic properties of binding—

To study the most prominent binding modes of the compounds in complex with the unamended and amended clays, we performed a statistical analysis on the interactions between the compounds and the clay layers within the simulations. Binding modes of the toxic compounds and the amending compound, carnitine, were classified based on decomposition of the toxic compounds and amending compound carnitine into functional groups, and were

clustered based on which functional groups independently or in combination bind to the clay, ultimately aiming to understand key mechanisms of binding. Both BPA and BPS were split into three functional groups, the two side aromatic groups both with an attached hydroxyl group, and the middle $-SO_2$ or $-C_3H_6$ groups, as illustrated in Fig. 3(A) and (B). DBP and DEHP were divided into one aromatic ring, two symmetric ester groups, and two symmetric carbon chain groups, as illustrated in Fig. 3(C) and (D). The amending compound, carnitine, was divided into three functional groups, the positively charged amine group and three attached methyl groups, the mid hydroxyl group and the linking carbon chain, and the carboxyl group, as illustrated in Fig. 3(E). Self-binding instances with unamended or amended clay were clustered into different binding modes depending on which functional groups of the toxic compounds, independently or in combinations, were binding to the clay layer. Assisted-binding instances with amended clay were classified into assisted-binding modes based on the functional groups of the amending compound, independently or in combinations, binding to the clay layer as well as the functional groups of toxic and amending compounds, independently or in combinations, interacting with each other based on the 3.5 Å cutoff. We calculated the percentage of binding modes given self-binding or assisted-binding such that the percentage of all self-binding modes sum up to unity and the percentage of all assisted-binding modes sum up to unity. Subsequently, we calculated the interaction energies of all self-binding modes with unamended clay as well as residence times of all self-binding modes with amended and unamended clay.

As the carboxylic group on the amending compound carnitine was frequently observed to form hydrogen bond with -OH groups present in BPA and BPS within the simulations, hydrogen bonding analysis was additionally conducted for the predominant assisted-binding mode of BPA and BPS, independently. Hydrogen bonding criterion was based on an angle cutoff of $> 120°$ and a hydrogen donor to acceptor distance cutoff of < 3.0 Å (Myers and Pace, 1996). Through this, we calculated the probabilities of BPA and BPS to form hydrogen bonds while adopting their predominant assisted-binding modes with carnitine.

2.3. Sorption isotherm experiments

Isothermal analysis was conducted followed by previous methods (Wang and Phillips, 2019). Briefly, 0.002% w/w of adsorbents were added to toxin solutions with an increasing gradient. Control groups included acetonitrile, BPA or DBP toxin solution without an adsorbent, and 0.002% adsorbent suspension.

From equilibrium isotherms, the toxin concentration in solution was detected, and the amount of toxin sorbed to the clays for each data point was calculated from the concentration difference between test and control groups. The best fit for these data was a Langmuir model, which was used to plot equilibrium isotherms from triplicate analysis. Parameters derived from the Langmuir equation coupled with the van't Hoff equation included binding capacity (Q_{max} in mol/kg), affinity (K_d), coefficient of determination (r^2), free energy (ΔG in kJ/mol), and enthalpy (ΔH in kJ/mol). Details of the experimental setup are presented in Supporting Material.

3. Results

3.1. Binding propensities of unamended and amended clays for the toxic compounds

3.1.1. Overall binding percentages and capacities—

The binding propensities of BPA, BPS, DBP, and DEHP to unamended and amended clays were computationally assessed, independently, through calculating the binding percentage within their respective simulations. Our computational analysis showed that BPA and BPS had higher binding propensities for both the unamended and amended clays compared to lower binding propensities for DBP and DEHP for both clays.

For the unamended clay, the binding percentages of BPA and BPS were 18% and 22%, respectively, and the binding percentages of DBP and DEHP were 8% and 5%, respectively (Fig. 4). Both BPA and BPS had high binding percentages for the unamended clay, with BPS having a higher binding percentage than BPA (Fig. 4). For the amended clay, the binding percentages of BPA and BPS were 39% and 42%, respectively, indicating that the carnitine amendments to the clay improved the binding of these toxic compounds. Conversely, the binding percentages of DBP and DEHP for the amended clay were 9% and 4%, respectively, indicating that the carnitine amendment to the clay did not improve their binding to the clay compared to their binding to the unamended clay.

Additionally, decomposition of the binding percentages of BPA and BPS binding to the amended clay into self- and assisted-binding showed that the assisted-binding percentage of BPS was lower than BPA, whereas the self-binding percentage of BPS was higher than BPA. Interestingly, the self-binding percentages of both BPA and BPS were higher for the amended clay compared to the unamended clay (Fig. 4). This suggests that the amended clay further enhances the direct binding of both toxic compounds to the clay, which will be discussed further in the following sections.

The experimental adsorption of BPA and DBP on clay surfaces as a function of their concentrations is shown in Fig. 5A and B. The curves from non-linear fitting with the experimental data are plotted and the corresponding parameters have been inserted in the table. The experimental equilibrium data for the sorption of BPA and DBP on both clays was best fit to the Langmuir model. This suggests the presence of homogeneous, saturable binding sites for both toxins. According to the Q_{max} parameters, the capacity of sorption on unamended and amended clays was more pronounced for BPA than for DBP, which is in good agreement with the binding percentages calculated through simulations shown in Fig. 4. Furthermore, the maximum adsorption capacity was enhanced by amended clay compared to the base clay for both BPA (0.29 mol/kg versus 0.25 mol/kg) and DBP (0.03 mol/kg and 0.01 mol/kg).

3.1.1.3. Additional insights into the overall binding propensities: The driving forces leading to the compounds' binding to unamended and amended clays were investigated through interaction energy calculations using simulation snapshots. The interaction energies of both BPA and BPS binding to either the unamended or amended clays were more energetically favorable compared to both DBP and DEHP; the strength of van der Waals interactions across all simulation systems was similar (Fig. 6). The interaction energies

decomposed into electrostatic and van der Waals components suggest that for BPA and BPS, electrostatic interactions play a key role for binding to both the unamended and amended clays. In addition, BPS had consistently more favorable electrostatic interaction energies compared to BPA when binding to either unamended or amended clay (Fig. 6).

The persistence of the compounds binding to unamended and amended clays were also investigated through calculating residence time of binding. The residence times of both BPA and BPS were significantly longer than the residence times of DBP and DEHP when binding to either the unamended or amended clay (Fig. S1). This could indicate that the binding of BPA and BPS was generally more persistent, which is in line with the higher binding percentages observed above. While the residence times of both BPA and BPS were longer when binding to the amended clay compared to the unamended clay, indicating that amendments improve the persistence of their binding, the residence times of DBP and DEHP were similar for amended and unamended clays (Fig. S1). This is in line with the lower binding percentages of DBP and DEHP for both unamended and amended clays (Fig. 4) and further suggests that carnitine-amendments would not greatly improve the binding of the phthalates. Interestingly, for unamended clay, BPS had a lower residence time than BPA, despite having a higher binding percentage, Fig. S1 (A). However, when binding to amended clay, BPS had a higher residence time than BPA in self-binding and assisted-binding, showing more persistent binding to amended clay, Fig. S1(B). The aforementioned computationally derived binding percentages, interaction energies, and residence times suggested that both the unamended and amended clays would have significantly higher binding capacities and affinities for BPA and BPS than for DBP and DEHP.

We experimentally assessed the feasibility of BPA and DBP sorption onto the clay surfaces through experimentally derived thermodynamic parameters. To calculate enthalpy of adsorption, isotherms of BPA and DBP binding onto amended clay were run at 37 °C and 24 °C, and derived K_d values were applied to the van't Hoff equation. As shown in Fig. 7A and B, it was noted that the ΔH (enthalpy) value was negative, indicating the feasibility of BPA and DBP binding to the clay. The calculated ΔH for BPA equals to −22.9 kJ/mol, suggesting tight binding at active surfaces on the clay. Importantly, this isothermal result is in alignment with the prediction that BPA is chemisorbed (electrostatically) to clay based on MD simulation studies. The calculated enthalpy for DBP binding onto amended clay from isothermal analysis showed significantly less sorption enthalpy than BPA ($\Delta H = -6.6$ kJ/mol for DBP). This isothermal result supports the MD simulation studies for DBP suggesting that weak physisorption mechanisms such as van der Waal's interactions may be the driving force for DBP binding. This finding can also account for the lower binding percentage, binding capacity, enthalpy and residence time of DBP. Experimentally derived isothermal data confirmed that the binding capacity and affinity of BPA was significantly higher than DBP. Thus, the subsequent analysis focuses on BPA and BPS only.

For the unamended clay, both BPA and BPS had high propensities to bind to the exterior of the clay within the simulations (Fig. 8). The percentages presented in Fig. 8 were calculated over the total number of binding instances by recording the probability of the binding instance to be at the exterior or interior of the clay. Compared to BPA, which was primarily bound to the exterior of the unamended clay, a significantly larger portion of BPS was bound

to the interior of the unamended clay (Fig. 8). The interior of the clay has a higher negative charge density compared to the exterior of the clay; thus, the partial positive charge of the sulfur in BPS could enhance its attraction to the negatively charged interior of the unamended clay, which will be discussed further in the following sections. For the amended clay, the percentage of BPS bound to the interior of the clay was still larger than that of BPA bound to the interior of the clay. Nonetheless, the presence of carnitine in the amended clay significantly increased the percentage of BPA self- and assisted-binding to the interior of the clay compared to the unamended clay (Fig. 8). This could be due to the fact that the positively charged carnitine was most frequently bound to the interior of the clay. For both unamended and amended clay, self-binding instances of BPA and BPS primarily occurred at the exterior of the clay (Fig. 8). SASA calculations of the clay atoms showed that oxygen atoms at the exterior of the clay had more than twice of the accessible area (SASA of 1.4 $Å^2$) of the oxygen atoms at the interior of the clay (SASA of 0.6 $Å^2$). Therefore, the oxygen atoms on the exterior of the clay are more exposed and amenable to participate in interactions with the toxic compounds compared to the oxygen atoms on the interior. The increased exposure of oxygen atoms at the exterior of clay could potentially play an important role in the mechanisms of self-binding for both BPA and BPS, as described in the binding mode analysis below. Nevertheless, the increased exposure of the oxygen atoms at the exterior of the clay modeled in the simulated systems could be overestimated compared to the naturally occurring clays, due to assumptions and limitations of the simulated modeled system.

3.2. Derivation of most populated binding modes within simulations and understanding their correlation to the structural and energetic properties of binding

We further aimed to obtain insights into the binding of BPA and BPS to the unamended and amended clays through deriving their Self- and assisted-binding modes. The binding modes were derived based on the decomposition of the toxic compounds and carnitine atoms into groups as shown in Fig. 3A,B,E. Fig. 9 presents the self-binding modes to unamended clay with their respective percentages, corresponding to the total number of instances in which the compound adopts one binding mode over the total number of binding instances. Fig. 10 presents the self-binding modes of the BPA and BPS binding to amended clay with their respective percentages, corresponding to the total number of instances in which the compound adopts one binding mode over the total number of binding instances.

For the unamended clay, both BPA and BPS were primarily bound through hydrogen bond interactions between oxygens of the clay and one hydroxyl group from BPA/BPS, referred to as the Aro binding mode (Fig. 9). For the predominant binding mode of BPA and BPS, the exterior oxygen atoms that are more exposed (as shown by the aforementioned SASA calculations) constituted sites for such hydrogen bonding. While BPA was bound to the clay almost entirely through the Aro binding mode (Fig. 9A), BPS also adopted additional binding modes with lower percentages (Fig. 9B). In these additional binding modes, BPS was bound to the clay through both its sulfur and hydroxyl groups simultaneously interacting with the clay, referred to as the Aro-Mid binding mode (Fig. 9B) or through both its hydroxyl groups forming hydrogen bonds with the clay, referred to as the Aro-Aro binding mode (Fig. 9B).

For the amended clay, the most predominant self-binding modes of BPA and BPS were nearly identical to their self-binding modes in complex with the unamended clay, forming hydrogen bonds with the oxygens of the clay through one of their hydroxyl group, referred to as the Aro binding mode (Fig. 10). While the composition of the prominent BPA self-binding modes to the amended clay was nearly the same as the percentage observed for BPA self-binding to the unamended clay (Fig. 11A), the prominent BPS self-binding modes in complex with the amended clay were less diverse than with the unamended clay (Fig. 11B). Nevertheless, in addition to the most prominent self-binding mode shared by both BPA and BPS binding to amended clay, BPS also bound to the clay with both hydroxyl groups interacting with the clay's exterior oxygen atoms, referred to as the Aro-Aro binding mode (Fig. 10B). The lower number of binding modes for BPS binding to amended clay compared to BPS binding to unamended clay could be due to the positively charged carnitine compounds occupying a significant space in the interior of the clay. I.e., the carnitine compounds, while allowing for assisted-binding of BPS, could impede to some extent BPS binding directly with the interior part of the clay.

We decomposed the self-binding modes of BPA and BPS in complex with unamended and amended clays into cases in which the compound was bound to the interior versus the exterior of the clay. Fig. 11 presents the percentages of all BPA and BPS self-binding modes with amended and unamended clays decomposed into interior and exterior binding. The percentage of BPA self-binding to the interior of the amended clay was larger compared to that of the unamended clay (Fig. 11). This could be due to BPA initially being involved in assisted-binding, which involves its interaction with a bound amending carnitine, and subsequently potentially transitioning into self-binding. As the amending carnitine compounds bind primarily with the clay interior, the likelihood of BPA being in proximity with the interior of the clay increases if it is initially involved in assisted-binding. Contrary to BPA, the self-binding modes of BPS occurred more frequently at the exterior of the amended clay compared to the unamended clay (Fig. 11B). This could indicate that BPS is less likely than BPA to transition from assisted-binding to self-binding, which is in line with the higher interior assisted-binding percentage of BPS compared to BPA (Fig. 8).

The predominant assisted-binding mode of both BPA and BPS in complex with the amended clay comprised of the toxic compounds interacting with bound amending carnitine compounds primarily via hydrogen bonding between the hydroxyl group of BPA or BPS and the carboxyl group of carnitine, referred to as Aro:Carbo (Fig. 12). Carnitine was bound to the clay interior via its positively charged amine group in over 90% of its binding instances. Additionally, despite the numerous combinations that could be possible between the interacting functional groups of carnitine with BPA/BPS, the clustering analysis showed only one highly predominant mode for both BPA and BPS assisted-binding to the amended clay. In the predominant assisted-binding mode, one hydroxyl group of BPA/BPS interacts with the carboxyl group of the bound amending carnitine (Aro:Carbo assisted-binding mode, Fig. 12). Of the instances of BPA and BPS adopting their predominant assisted-binding modes, a hydrogen bond was formed between BPA or BPS and carnitine in approximately 65% of the cases, which is relatively high considering the relatively strict hydrogen bonding criterion used. All other assisted-binding modes occurred infrequently, and both BPA and BPS adopted only one predominant assisted-binding mode.

We compared the electrostatic and van der Waals interaction energies of the different self-binding modes of BPA and BPS in complex with the unamended clays (Fig. 13). The electrostatic interaction energies of BPS were more favorable than those of BPA across all modes except for the Aro-Mid binding mode (Fig. 13). It is worth noting that the electrostatic energy of BPA's Aro-Mid binding mode had a relatively high standard error, indicating potentially high variability of the interactions formed by the compound and the clay in such modes and low statistical significance; this is in line with visual inspection of simulation snapshots comprising BPA adopting the Aro-Mid binding mode. The more favorable electrostatic interaction energies for the self-binding modes of BPS compared to BPA indicated that the partially positive sulfur of BPS could be associated with the higher binding propensities of BPS compared to BPA. Given that electrostatic interaction is longer range than van der Waals, even in binding modes in which the Mid functional group of BPS was not in contact with the clay (as in the Aro and Aro-Aro binding modes, both with high interior percentage via hydrogen bonding of the hydroxyl group(s) of BPS), BPS had higher electrostatic interaction energies compared to BPA (Fig. 13). Interestingly, for both BPA and BPS, the Aro-Aro binding mode had the most favorable interaction energy followed by the Aro binding mode despite the Aro binding mode being the predominantly formed binding mode for both compounds (Figs. 11 and 13). The higher percentage of BPA and BPS forming the Aro binding mode compared to the Aro-Aro binding mode could be due to the Aro binding mode requiring the formation of only one hydrogen bond rather than the two hydrogen bonds needed in the Aro-Aro binding mode. This could additionally indicate that BPA and BPS first form the Aro binding mode and then transition into the Aro-Aro binding mode.

We additionally compared the residence times of different binding modes of BPA and BPS in complex with the unamended and amended clays (Fig. S2A). For the unamended clay, the predominant self-binding mode of both BPA and BPS, in which one hydroxyl group of BPA/BPS interacted with the clay (the Aro binding mode, Fig. 9), had the longest residence times compared to all other self-binding modes (Fig. S2A). Additionally, in the predominant self-binding mode, the Aro binding mode (Fig. 9), BPA had a longer residence time than BPS (Fig. S2A). This is reflected in the overall longer residence time of BPA in any binding mode compared to BPS (Fig. S1A). However, the residence times of BPS adopting self-binding modes Aro, Aro-Aro, and Aro-Mid, with unamended clay, were longer than the residence times of BPA in the same, corresponding self-binding modes (Fig. S2A). The overall shorter residence time and higher propensity of binding for BPS binding to the unamended clay compared to BPA could be due to the diversity of BPS self-binding modes with unamended clay (Figs. 9 and 11) resulting in more relatively transient self-binding modes. These relatively transient self-binding modes could be linked to a decrease in residence time, but higher overall binding propensity. For the amended clay, the predominant self-binding mode of both BPA and BPS, the Aro binding mode (Fig. 10), also had the longest residence times compared to all other self-binding modes (Fig. S2B). For BPA, the residence times of self-binding modes in complex with unamended clay and amended clay were similar (Fig. S2A). This could be expected as the composition of self-binding modes of BPA are similar for both amended and unamended clays (Fig. 11A). For BPS, the residence times of the predominant self-binding modes, Aro and Aro-Aro binding modes (Figs. 9 and

10), were longer when in complex with the amended clay than with the unamended clay (Fig. S2B). This could be due to the lower diversity of self-binding modes (Figs. 9B and 11B), resulting in less transient self-binding modes and longer residence times.

4. Conclusion

In this study, we have computationally and experimentally characterized the binding and sorption of BPA and BPS (common precursors of plastics) and DBP and DEHP (important plasticizers) to active surfaces within the interlayer (internal) and on basal surfaces (external) of montmorillonite clays. We computationally used distance-based geometric criteria which enabled us to both understand the overall binding propensities of different compounds in complex with unamended and amended clays, as well as to classify the structural properties among different binding modes of the molecules. Interaction energy analysis was additionally used to primarily reveal the strength of interaction and the driving forces of binding. Compared with our previous clay studies with pesticides (Wang et al., 2019), here we expanded the computational methods, and aimed to provide insights into the molecular mechanisms of BPA, BPS, DBP, and DEHP binding to unamended and nutrient (carnitine-)amended clays. Despite any approximations of the modeled simulated systems, including (1) the higher concentrations of toxic compounds which aimed to enhance the statistical sampling and accelerate the potential sorption of toxic compounds to the clay surfaces within the simualtions (Wang et al., 2019; Tamamis et al., 2009; Chen et al., 2020; Tao et al., 2020; Wang et al., 2017; Wang et al., 2016), (2) the potential overestimation of edge binding sites on the clay compared to the natural clay which is an artifact of the modeled system, and (3) the non-usage of any umbrella sampling method in the simulations which could facilitate the exploration of different binding modes (Tamamis et al., 2009; Tamamis et al., 2014; Tamamis et al., 2009; Palmer et al., 2013; Zerze et al., 2020; Depaepe et al., 1993; O'Connor et al., 2016; Northrup et al., 1982; Berg and Neuhaus, 1992; Wang and Landau, 2001; Oshima et al., 2019), simulation and analysis procedure used in this study provided reasonably high qualitative correlations between computations and experiments. Particularly, these qualitative comparisons were used to delineate toxic compounds that can be effectively sorbed onto the clay (BPA and BPS) from those that cannot (DBP and DEHP). Additionally, interaction energy calculations indicated the strength of interaction of the toxic compounds to the clay and showed that electrostatic interactions are the key driving force leading to BPA and BPS sorption onto the clay. Importantly, simulating the toxic compounds in higher concentrations compared to experiments (Wang et al., 2019; Tamamis et al., 2009; Chen et al., 2020; Tao et al., 2020; Wang et al., 2017; Wang et al., 2016), and the use relatively simple serial MD runs compared to more costly umbrella sampling techniques has proven beneficial in terms of efficiency and accuracy in this study and provided the impetus for ongoing and future larger-scale studies of our labs exploiting relatively low-cost simulations and interaction energy calculations for the derivation of data-driven semi-empirical models (Kozuch et al., 2018; Khoury et al., 2017; Kieslich et al., 2016; Shockey et al., 2019) quantitatively predicting experimental data and distinguishing between high vs. low affinity toxic compound binders to montmorillonite clays (unpublished work).

Here, we have shown that an amended montmorillonite clay is capable of significantly binding BPA and BPS with high affinity, high capacity and high enthalpy. Thus, it is possible that this clay, which is similar to the edible clay used for aflatoxin mitigation, could be further investigated in the future to potentially serve as a supplement in food and water to decrease the bioavailability of these contaminants and reduce the adverse health effects from unintentional exposures. Optimal toxin sorbents which can be designed through molecular simulations and isothermal analyses could, upon further investigation in future studies, potentially be included in food (such as snacks), condiments, and flavored water, or delivered by sachet or capsule as therapy for important environmental contaminants. Importantly, future studies are warranted to confirm the efficacy of this clay *in vivo*.

Supplementary Material

Refer to Web version on PubMed Central for supplementary material.

Acknowledgments

The authors acknowledge support from the Superfund Hazardous Substance Research and Training Program (National Institutes of Health), P42 ES027704. All MD simulations were performed on the Ada supercomputing cluster at the Texas A&M High Performance Research Computing center.

References

Aggarwal V, Chien Y-Y, Teppen BJ, 2007 Molecular simulations to estimate thermodynamics for adsorption of polar organic solutes to Montmorillonite. Eur. J. Soil Sci. 58, 945–957. doi:10.1111/j.1365-2389.2007.00939.x.

Akingbemi BT, Ge R, Klinefelter GR, Zirkin BR, Hardy MP, 2004 Phthalate-induced Leydig cell hyperplasia is associated with multiple endocrine disturbances. Proc. Natl Acad. Sci. 101, 775–780. doi:10.1073/pnas.0305977101. [PubMed: 14715905]

Andrady LA, Neal MA, 2009 Applications and societal benefits of plastics. Philos. Trans. R. Soc. Lond. B Biol. Sci. 364 (1526), 1977–1984. doi:10.1098/rstb.2008.0304. [PubMed: 19528050]

Aristilde L, Marichal C, Miéhé-Brendlé J, Lanson B, Charlet L, 2010 Interactions of oxytetracycline with a smectite clay: a spectroscopic study with molecular simulations. Environ. Sci. Technol. 44, 7839–7845. doi:10.1021/es102136y. [PubMed: 20866047]

Asada T, Oikawa K, Kawata K, et al., 2004 Study of removal effect of bisphenol A and & β-estradiol by porous carbon. J. Health Sci. 50 (6), 588–593. doi:10.1248/jhs.50.588.

Awuor AO, Yard E, Daniel JH, Martin C, Bii C, Romoser A, Oyugi E, Elmore S, Amwayi S, Vulue J, Zitomer NC, Rybak ME, Phillips TD, Montgomery JM, Lewis LS, 2017 Evaluation of the efficacy, acceptability and palatability of calcium montmorillonite clay used to reduce aflatoxin B1 dietary exposure in a crossover study in Kenya. Food Addit. Contam. 34, 93–102. doi:10.1080/19440049.2016.1224933.

Berg BA, Neuhaus T, 1992 Multicanonical ensemble: a new approach to simulate first-order phase transitions. Phys. Rev. Lett. 68 (1), 9–12. doi:10.1103/PhysRevLett.68.9. [PubMed: 10045099]

Betts KS, 2011 Plastics and food sources: dietary intervention to reduce BPA and DEHP. Environ. Health Perspect. 119 (7), A306. doi:10.1289/ehp.119-a306b.

Bloom MS, Whitcomb BW, Chen Z, Ye A, Kannan K, Buck Louis GM, 2015 Associations between urinary phthalate concentrations and semen quality parameters in a general population. Hum. Reprod. 30 (11), 2645–2657. doi:10.1093/humrep/dev219. [PubMed: 26350610]

Bošnir J, Puntarić D, Galić A, Škes I, Dijanić T, Klarić M, et al., 2007 Migration of phthalates from plastic containers into soft drinks and mineral water. Food Technol. Biotechnol. 45, 91–95.

Bodzeka M, Dudziaka M, Luks-Betlejb K, 2004 Application of membrane techniques to water purification. Removal of phthalates.. Desalination. 162, 121–128. doi:10.1016/S0011-9164(04)00035-9.

Bonna RJ, Aulerich RJ, Bursian SJ, Poppenga RH, Braselton WE, Watson GL, 1991 Efficacy of hydrated sodium calcium aluminosilicate and activated charcoal in reducing the toxicity of dietary aflatoxin to mink. Arch. Environ. Contam. Toxicol. 20, 441–447. doi:10.1007/BF01064418. [PubMed: 1650170]

Boscolo Boscoletto A, Gottardi F, Pannocchia P, Tartari V, Tavan M, Amadelli R, De Battisti A, Barbieri A, Patracchini D, Battaglin G, 1994 Electrochemical treatment of bisphenol-A containing wastewaters. J. Appl. Electrochem. 10, 1052–1058. doi:10.1007/BF00241198.

Braun JM, Sathyanarayana S, Hauser R, 2013 Phthalate exposure and children's health. Curr. Opin. Pediatr. 25 (2), 247–254. doi:10.1097/MOP.0b013e32835e1eb6. [PubMed: 23429708]

Brooks BR, Brooks CL 3rd, Mackerell AD Jr, Nilsson L, Petrella RJ, Roux B, Won Y, Archontis G, Bartels C, Boresch S, Caflisch A, Caves L, Cui Q, Dinner AR, Feig M, Fischer S, Gao J, Hodoscek M, Im W, Kuczera K, Lazaridis T, Ma J, Ovchinnikov V, Paci E, Pastor RW, Post CB, Pu JZ, Schaefer M, Tidor B, Venable RM, Woodcock HL, Wu X, Yang W, York DM, Karplus M, 2009 CHARMM: the biomolecular simulation program. J. Comput. Chem. 30 (10), 1545–1614. doi:10.1002/jcc.21287. [PubMed: 19444816]

Brotons JA, Oleaserrano MF, Villalobos M, Pedraza V, Olea N, 1995 Xenoestrogens released from lacquer coatings in food cans. Environ. Health Perspect. 103, 608–612. doi:10.1289/ehp.95103608. [PubMed: 7556016]

Centers for Disease Control and Prevention., 2018 Fourth report on human exposure to environmental chemicals, updated tables. Atlanta, GA: U.S.Department of Health and Human Services, Centers for Disease Control and Prevention https://www.cdc.gov/exposurereport/ (accessed 4 September 2018).

Chang W-H, Li S-S, Wu M-H, Pan H-A, Lee C-C, 2015 Phthalates might interfere with testicular function by reducing testosterone and insulin-like factor 3 levels. Hum. Reprod. 30 (11), 2658–2670. doi:10.1093/humrep/dev225. [PubMed: 26385792]

Chen MY, Ike M, Fujita M, 2002 Acute toxicity, mutagenicity, and estrogenicity of bisphenol-A and other bisphenols. Environ. Toxicol. 17 (1), 80–86. doi:10.1002/tox.10035. [PubMed: 11847978]

Chen CY, Wu PS, Chung YC, 2009 Coupled biological and photo-Fenton pretreatment system for the removal of di-(2-ethylhexyl) phthalate (DEHP) from water. Bioresour. Technol. 100 (19), 4531–4534. doi:10.1016/j.biortech.2009.04.020. [PubMed: 19423337]

Chen Y, Shu L, Qiu Z, Lee DY, Settle SJ, Hee SQ, Telesca D, Yang X, Allard P, 2016 Exposure to the BPA-substitute bisphenol S causes unique alterations of germline function. PLos Genet. 127, e1006223. doi:10.1371/journal.pgen.1006223.

Chen Y, Orr AA, Tao K, Wang Z, Ruggiero A, Shimon LJW, Schnaider L, Goodall A, Rencus-Lazar S, Gilead S, Slutsky I, Tamamis P, Tan Z, Gazit E.., 2020 High-efficiency fluorescence through bioinspired supramolecular self-assembly. ACS Nano 14 (3), 2798–2807. doi:10.1021/acsnano.9b10024. [PubMed: 32013408]

Chou K, Wright RO, 2006 Phthalates in food and medical devices. J. Med. Toxicol. 2, 126–135. doi:10.1007/BF03161027. [PubMed: 18077888]

Clewell RA, Campbell JL, Ross SM, Gaido KW, Clewell HJ, Andersen ME, 2010 Assessing the relevance of in vitro measures of phthalate inhibition of steroidogenesis for in vivo response. Toxicol. Vitro 24 (1), 327–334. doi:10.1016/j.tiv.2009.08.003.

Colvin RM, Sangster LT, Hayden KD, Bequer RW, Wiln DM, 1989 Effect of high affinity aluminosilicate sorbent on prevention of aflatoxicosis in growing pigs. Vet. Hum. Toxicol. 31, 46–48. [PubMed: 2711607]

Cruz-Guzmán M, Celis R, Hermosín MC, Cornejo J, 2004 Adsorption of the herbicide simazine by montmorillonite modified with natural organic cations. Environ. Sci. Technol. 38 (1), 180–186. doi:10.1021/es030057w. [PubMed: 14740734]

Cruz-Guzmán M, Celis R, Hermosín MC, Cornejo J, 2004 Adsorption of the herbicide simazine by montmorillonite modified with natural organic cations. Environ. Sci. Technol. 38 (1), 180–186. doi:10.1021/es030057w. [PubMed: 14740734]

Depaepe J-M, Ryckaert J-P, Paci E, Ciccotti G, 1993 Sampling of molecular conformations by molecular dynamics techniques. Mol. Phys. 79 (3), 515–522. doi:10.1080/00268979300101411.

Emami FS, Puddu V, Berry RJ, Varshney V, Patwardhan SV, Perry CC, Heinz H, 2014 Prediction of specific biomolecule adsorption on silica surfaces as a function of ph and particle size. Chem. Mater. 26, 5725–5734. doi:10.1021/cm5026987.

Feng Y, Jiao Z, Shi J, Li M, Guo Q, Shao B, 2016 Effects of bisphenol analogues on steroidogenic gene expression and hormone synthesis in H295R cells. Chemosphere 147, 9–19. doi:10.1016/j.chemosphere.2015.12.081. [PubMed: 26751127]

Gözmen B, Oturan MA, Oturan N, Erbatur O, 2003 Indirect electrochemical treatment of bisphenol A in water via electrochemically generated Fenton's reagent. Environ. Sci. Technol. 37 (16), 3716–3723. doi:10.1021/es034011e. [PubMed: 12953886]

Gray LE Jr., Barlow NJ, Howdeshell KL, Ostby JS, Furr JR, Gray CL, 2009 Transgenerational effects of di (2-ethylhexyl) phthalate in the male CRL:CD(SD) rat: added value of assessing multiple offspring per litter. Toxicol. Sci. 110, 411–425. doi:10.1093/toxsci/kfp109. [PubMed: 19482887]

Grindler NM, Vanderlinden L, Karthikraj R, et al., 2018 Exposure to phthalate, an endocrine disrupting chemical, alters the first trimester placental methylome and transcriptome in women. Sci. Rep. 8, 6086. doi:10.1038/s41598-018-24505-w. [PubMed: 29666409]

Héliès-Toussaint C, Peyre L, Costanzo C, Chagnon M-C, Rahmani R, 2014 Is bisphenol S a safe substitute for bisphenol A in terms of metabolicfunction? An in vitro study. Toxicol. Appl. Pharmacol. 280, 224–235. doi:10.1016/j.taap.2014.07.025. [PubMed: 25111128]

Halden RU, 2010 Plastics and health risks. Annu. Rev. Public Health 31, 179–194. doi:10.1146/annurev.publhealth.012809.103714. [PubMed: 20070188]

Harvey R, Kubena LF, Phillips TD, Corrier DE, Elissalde MH, Huff WE, 1991 Diminution of aflatoxin toxicity to growing lambs by dietary supplementation with hydrated sodium calcium aluminosilicate. Am. Vet. Res. 52, 152–156.

Harvey RB, Phillips TD, Ellis JA, Kubena LF, Huff WE, Petersen DV, 1991 Effects of aflatoxin M residues in milk by addition of hydrated sodium calcium aluminosilicate to aflatoxin contaminated diets of dairy cows. Am. J. Vet. Res. 52, 1556–1559. [PubMed: 1659263]

Harvey R, Kubena LF, Elissalde M, Corrier D, Phillips TD, 1994 Comparison of two hydrated sodium calcium aluminosilicate compounds to experimentally protect growing barrows from aflatoxicosis. Vet. Diagn. Invest. 6, 88–92. doi:10.1177/104063879400600115.

He PJ, Zheng Z, Zhang H, Shao LM, Tang QY, 2009 PAEs and BPA removal in landfill leachate with Fenton process and its relationship with leachate DOM composition. Sci. Total Environ. 407 (17), 4928–4933. doi:10.1016/j.scitotenv.2009.05.036. [PubMed: 19520416]

Hearon SE, Wang M, Phillips TD, 2020 Strong adsorption of dieldrin by parent and processed montmorillonite clays. Environ. Toxicol. Chem. 39 (3), 517–525. doi:10.1002/etc.4642. [PubMed: 31756776]

Heinz H, Koerner H, Adnerson KL, Vaia RA, Farmer BL, 2005 Force field for micatype silicates and dynamics of octadecylammonium chains grafted to montmorillonite. Chem. Mater. 17, 5658–5669. doi:10.1021/cm0509328.

Heinz H, Vaia RA, Farmer BL, 2006 Interaction energy and surface reconstruction between sheets of layered silicates. J. Chem. Phys. 124 (22), 224713. doi:10.1063/1.2202330. [PubMed: 16784307]

Heinz H, Lin TJ, Mishra RK, Emami FS, 2013 Thermodynamically consistent force fields for the assembly of inorganic, organic, and biological nanostructures: the interface force field. Langmuir 29, 1754–1765. doi:10.1021/la3038846. [PubMed: 23276161]

Hu GX, Lian QQ, Ge RS, Hardy DO, Li XK, 2009 Phthalate-induced testicular dysgenesis syndrome: leydig cell influence. Trends Endocrinol. Metab. 20 (3), 139–145. doi:10.1016/j.tem.2008.12.001. [PubMed: 19278865]

Huang J, MacKerell AD, 2013 CHARMM36 all-atom additive protein force field: validation based on comparison to NMR data. J. Comput. Chem. 34 (25), 2135–2145. doi:10.1002/jcc.23354. [PubMed: 23832629]

Im W, Lee MS, Brooks CL, 2003 Generalized born model with a simple smoothing function. J. Comput. Chem. 24, 1691–1702. doi:10.1002/jcc.10321. [PubMed: 12964188]

Jayaprakash M, Gowda RNS, Vijayasarathi SK, Seshadri SI, 1992 Adsorbent efficacy of hydrated sodium calcium aluminosilicate in induced aflatoxicosis in broilers. Indian J. Vet. Pathol. 16, 102. doi:10.3382/ps.2012-02510.

Jaynes WF, Boyd SA, 1991 Hydrophobicity of siloxane surfaces in smectites as revealed by aromatic hydrocarbon adsorption from water. Clays Clay Miner. 39, 428–436. doi:10.1346/CCMN.1991.0390412.

Jensen MS, Nørgaard-Pedersen B, Toft G, Hougaard DM, Bonde JP, Cohen A, Thulstrup AM, Ivell R, Anand-Ivell R, Lindh CH, Jönsson BA, 2012 Phthalates and perfluorooctanesulfonic acid in human amniotic fluid: temporal trends and timing of amniocentesis in pregnancy. Environ. Health Perspect. 120 (6), 897–903. doi:10.1289/ehp.1104522. [PubMed: 22398305]

Kang JH, Kito K, Kondo F, 2003 Factors influencing the migration of bisphenol A from cans. J. Food Prot. 66, 1444–1447. doi:10.4315/0362-028x-66.8.1444. [PubMed: 12929833]

Khoury GA, Smadbeck J, Kieslich CA, Koskosidis AJ, Guzman YA, Tamamis P, Floudas CA, 2017 Princeton_TIGRESS 2.0: high refinement consistency and net gains through support vector machines and molecular dynamics in double-blind predictions during the CASP11 experiment. Proteins 85 (6), 1078–1098. doi:10.1002/prot.25274. [PubMed: 28241391]

Kieslich CA, Smadbeck J, Khoury GA, Floudas CA, 2016 conSSert: consensus SVM model for accurate prediction of ordered secondary structure. J. Chem. Inf. Model. 56 (3), 455–461. doi:10.1021/acs.jcim.5b00566. [PubMed: 26928531]

Kolla S, Morcos M, Martin B, Vandenberg LN, 2018 Low dose bisphenol S or ethinyl estradiol exposures during the perinatal period alter female mouse mammary gland development. Reprod. Toxicol. 78, 50–59. doi:10.1016/j.reprotox.2018.03.003. [PubMed: 29526645]

Konieczna A, Rutkowska A, Rachoń D, 2015 Health risk of exposure to Bisphenol A (BPA). Rocz. Panstw. Zakl. Hig. 66 (1), 5–11. [PubMed: 25813067]

Kovačič A, Gys A, Kosjek T, Covaci A, Heath E, 2019 Photochemical degradation of BPF, BPS and BPZ in aqueous solution: identification of transformation products and degradation kinetics. Sci. Total Environ. 664, 595–604. doi:10.1016/j.scitotenv.2019.02.064. [PubMed: 30763840]

Kozuch DJ, Stillinger FH, Debenedetti PG, 2018 Combined molecular dynamics and neural network method for predicting protein antifreeze activity. PNAS 115 (52), 13252–13257. doi:10.1073/pnas.1814945115. [PubMed: 30530650]

Kristof T, Sarkadi Z, Hato Z, Rutkai G, 2018 Simulation study of intercalation complexes of kaolinite with simple amides as primary intercalation reagents. Comput. Mater. Sci. 143, 118. doi:10.1016/j.commatsci.2017.11.010.

Kubena LF, Harvey RB, Phillips TD, Corrier DE, Huff WE, 1990 Diminution of aflatoxicosis in growing chickens by dietary addition of a hydrated sodium calcium aluminosilicate. Poultry Sci. 69, 727–735. doi:10.3382/ps.0690727. [PubMed: 1973286]

Kubena LF, Huff WE, Harvey RB, Yersin AG, Elissalde MH, Witzel DA, Giroir LE, Phillips TD, 1991 Effects of hydrated sodium calcium aluminosilicate on growing turkey poults during aflatoxicosis. Poultry Sci. 70, 1823–1830. doi:10.3382/ps.0701823. [PubMed: 1656420]

Kubena LF, Harvey RB, Huff WE, Yersin AG, Elissalde MH, Witzel DA, 1993 Efficacy of a hydrated sodium calcium aluminosilicate to reduce the toxicity of aflatoxin and diacetoxyscirpenol. Poultry Sci. 72, 51–59. doi:10.3382/ps.0720051. [PubMed: 8381229]

Kubwabo C, Kosarac I, Stewart B, Gauthier BR, Lalonde K, Lalonde PJ, 2009 Migration of bisphenol A from plastic baby bottles, baby bottle liners and reusable polycarbonate drinking bottles. Food Additives & Contaminants. Part A. Chem., Anal., Control, Expo. Risk Assess. 26 (6), 928–937. doi:10.1080/02652030802706725.

López-Ramón MV, Ocampo-Pérez R, Bautista-Toledo MI, Rivera-Utrilla J, Moreno-Castilla C, Sánchez-Polo M, 2019 Removal of bisphenols A and S by adsorption on activated carbon clothes enhanced by the presence of bacteria. Sci. Total Environ. 669, 767–776. doi:10.1016/j.scitotenv.2019.03.125. [PubMed: 30897435]

Lang IA, Galloway TS, Scarlett A, Henley WE, Depledge M, Wallace RB, Melzer D, 2008 Association of urinary bisphenol A concentration with medical disorders and laboratory abnormalities in adults. JAMA 300 (11), 1303–1310. doi:10.1001/jama.300.11.1303. [PubMed: 18799442]

Li SZ, Wu PX, 2010 Characterization of sodium dodecyl sulfate modified iron pillared montmorillonite and its application for the removal of aqueous Cu(II) and Co(II). J. Hazard. Mater. 173 (1–3), 62–70. doi:10.1016/j.jhazmat.2009.08.047,2010. [PubMed: 19748730]

Liaqat I, 2018 Interactions between bisphenol s or dibutyl phthalates and reproductive system. Endocrine Disruptors, Ahmed R. G., IntechOpen doi:10.5772/intechopen.79264.

Lindemann MD, Blodgett DJ, Kornegay ET, Schurig GG, 1993 Potential ameliorators of aflatoxicosis in weanling/growing swine. J. Anim. Sci. 71, 171–178. doi:10.2527/1993.711171x. [PubMed: 8384193]

Lioy PJ, Hauser R, Gennings C, Koch HM, Mirkes PE, Schwetz BA, Kortenkamp A, 2015 Assessment of phthalates/phthalate alternatives in children's toys and childcare articles: review of the report including conclusions and recommendation of the Chronic Hazard Advisory Panel of the Consumer Product Safety Commission. J. Expo. Sci. Environ. Epidemiol. 25 (4), 343–353. doi:10.1038/jes.2015.33. [PubMed: 25944701]

Liu G, Ma J, Li X, et al., 2009 Adsorption of bisphenol A from aqueous solution onto activated carbons with different modification treatments. J. Haz. Mat. 164 (2–3), 1275–1280. doi:10.1016/j.jhazmat.2008.09.038.

Maki CR, Haney S, Wang M, Ward SH, Rude BJ, Bailey RH, Harvey RH, Phillips TD, 2017 Calcium Montmorillonite clay for the reduction of aflatoxin residues in milk and dairy products. J. Diary Vet. Sci. 2, 555587. doi:10.19080/JDVS.2017.02.555587.

Mako E, Kovacs A, Hato Z, Zsirka B, Kristof T, 2014 Characterization of kaolinite-ámmonium acetate complexes prepared by one-step homogenization method. J. Colloid Interface Sci. 431, 125–131. doi:10.1016/j.jcis.2014.06.006. [PubMed: 24996021]

Mersha MD, Patel BM, Patel D, Richardson BN, Dhillon HS, 2015 Effects of BPA and BPS exposure limited to early embryogenesis persist to impair non-associative learning in adults. Behav. Brain Funct. 11, 27. doi:10.1186/s12993-015-0071-y. [PubMed: 26376977]

Michaud-Agrawal N, Denning EJ, Woolf TB, Beckstein O, 2011 MDAnalysis: a toolkit for the analysis of molecular dynamics simulations. J. Comput. Chem. 32 (10), 2319–2327. doi:10.1002/jcc.21787. [PubMed: 21500218]

Mihucz VG, Záray G, 2016 Occurrence of antimony and phthalate esters in polyethylene terephthalate bottled drinking water. Appl. Spectros. Rev. 51, 183–209. doi:10.1080/05704928.2015.1105243.

Mitchell NJ, Kumi J, Aleser M, Elmore SE, Rychlik KA, Zychowski KE, Romoser AA, Phillips TD, Ankrah NA, 2014 Short-term safety and efficacy of calcium montmorillonite clay (USPN) in children. Am. J. Trop. Med. Hyg. 91, 777–785. doi:10.4269/ajtmh.14-0093. [PubMed: 25135766]

Mohan SV, Shailaja S, Krishna MR, Sarma PN, 2007 Adsorptive removal of phthalate ester (Di-ethyl phthalate) from aqueous phase by activated carbon: a kinetic study. J. Haz. Mater. 146, 278–282. doi:10.1016/j.jhazmat.2006.12.020.

Moon MK, 2019 Concern about the safety of bisphenol A substitutes. Diabetes Metab. J. 43 (1), 46–48. doi:10.4093/dmj.2019.0027. [PubMed: 30793551]

Myers JK, Pace CN, 1996 Hydrogen bonding stabilizes globular proteins. Biophys. J. 71 (4), 2033–2039. doi:10.1016/S0006-3495(96)794018. [PubMed: 8889177]

Nakanishi A, Tamai M, Kawasaki N, et al., 2002 Adsorption characteristics of bisphenol A onto carbonaceous materials produced from wood chips as organic waste. J. Colloid Interface Sci. 252 (2), 393–396. doi:10.1006/jcis.2002.8387. [PubMed: 16290804]

North EJ, Halden RU, 2013 Plastics and environmental health: the road ahead. Rev. Environ. Health 28 (1), 1–8. doi:10.1515/reveh-2012-0030. [PubMed: 23337043]

Northrup SH, Pear MR, Lee CY, McCammon JA, Karplus M, 1982 Dynamical theory of activated processes in globular proteins. Proc. Natl. Acad. Sci. 79 (13), 4035–4039. doi:10.1073/pnas.79.13.4035. [PubMed: 6955788]

O'Connor M, Paci E, McIntosh-Smith S, Glowacki DR, 2016 Adaptive free energy sampling in multidimensional collective variable space using boxed molecular dynamics. Faraday Discuss. 195, 395–419. doi:10.1039/c6fd00138f. [PubMed: 27738687]

Olea N, Pulgar R, Perez P, Olea-Serrano F, Rivas A, et al., 1996 Estrogenicity of resin-based composites and sealants used in dentistry. Environ. Health Perspect. 104, 298–305. doi:10.1289/ehp.96104298. [PubMed: 8919768]

Ortiz-Zarragoitia M, Trant JM, Cajaravillet MP, 2006 Effects of dibutylphthalate and ethynylestradiol on liver peroxisomes, reproduction, and development of zebrafish (Danio rerio). Environ. Toxicol. Chem. 25 (9), 2394–2404. doi:10.1897/05-456r.1. [PubMed: 16986795]

Oshima H, Re S, Sugita Y, 2019 Replica-exchange umbrella sampling combined with gaussian accelerated molecular dynamics for free-energy calculation of biomolecules. J. Chem. Theory Comput. 15 (10), 5199–5208. doi:10.1021/acs.jctc.9b00761. [PubMed: 31539245]

Pacella MS, Gray JJ, 2018 A benchmarking study of peptide-biomineral interactions. Cryst. Growth Des. 18, 607–616. doi:10.1021/acs.cgd.7b00109.

Palmer JC, Car R, Debenedetti PG, 2013 The liquid-liquid transition in supercooled ST2 water: a comparison between umbrella sampling and well-tempered metadynamics. Faraday Discuss. 167, 77. doi:10.1039/c3fd00074e. [PubMed: 24640486]

Phillips TD, Clement BA, Kubena LF, Harvey RB, 1990 Detection and detoxification of aflatoxins: prevention of aflatoxicosis and aflatoxin residues with hydrated sodium calcium aluminosilicates. Vet. Human. Toxicol. 32, 15–19.

Phillips TD, Sarr AB, Clement BA, Kubena LF, Harvey RB, 1991 Prevention of aflatoxicosis in farm animals via selective chemisorption of aflatoxin. In: Bray GA, Ryan DH (Eds.), Mycotoxins, Cancer and Health. Louisiana State University Press, Baton Rouge, p. 1.

Phillips TD, Clement BA, Park DL, 1994 Approaches to reduction of aflatoxin In: Eaton LD, Groopman JD (Eds.), In The Toxicology of Aflatoxins, Human Health, Veterinary Agricultural Significance. Academic Press, NY doi:10.1016/B978-0-12-228255-3.50023-4.

Phillips TD, Sarr AB, Grant PG, 1995 Selective chemisorption and detoxification of aflatoxins by phyllosilcate clay. Nat. Toxins. 3, 204–213. doi:10.1002/nt.2620030407. [PubMed: 7582618]

Phillips TD, Wang M, Elmore SE, Hearon S, Wang J-S, 2019 NovaSil Clay for the protection of humans and animals from aflatoxins and other contaminants. Clays Clay Miner. 67, 99–110. doi:10.1007/s42860-019-0008-x. [PubMed: 32943795]

Pjanic M, 2017 The role of polycarbonate monomer bisphenol-A in insulin resistance. PeerJ 5, e3809. doi:10.7717/peerj.3809. [PubMed: 28929027]

Pollock BH, Elmore S, Romoser A, Tang L, Kang MS, Xue K, Rodriguez M, Dierschke NA, Hayes HG, Hansen HA, 2016 Intervention trial with calcium montmorillonite clay in a south Texas population exposed to aflatoxin. Food Addit. Contam. 33, 1346–1354. doi:10.1080/19440049.2016.1198498.

Prasanth GK, Divya LM, Sadasivan C, 2009 Effects of mono and di(n-butyl) phthalate on superoxide dismutase. Toxicology 262 (1), 38–42. doi:10.1016/j.tox.2009.04.036. [PubMed: 19386278]

Ramesh V, Biswal M, Mohanty S, Nayak SK, 2014 Recycling of engineering plastics from waste electrical and electronic equipments: influence of virgin polycarbonate and impact modifier on the final performance of blends. Waste Manag. Res. 32 (5), 379–388. doi:10.1177/0734242X14528404. [PubMed: 24695435]

Ritter S, 2011 BPA is indispensible for making plastics. Chem. Eng. News 89 https://pubs.acs.org/cen/coverstory/89/8923cover4.html. accessed 6 August 2018.

Rosenmai AK, Dybdahl M, Pedersen M, Alice van Vugt-Lussenburg BM, Wedebye EB, Taxvig C, Vinggaard AM, 2014 Are structural analogues to bisphenol a safe alternatives? Toxicol. Sci. 139 (1), 35–47. doi:10.1093/toxsci/kfu030. [PubMed: 24563381]

Russo G, Barbato F, Cardone E, Fattore M, Albrizioa S, Grumetto L, 2018 Bisphenol A and Bisphenol S release in milk under household conditions from babybottles marketed in Italy. J. Environ. Sci. Health B 53 (2), 116–120. doi:10.1080/03601234.2017.1388662. [PubMed: 29172986]

Rusyn I, Peters JM, Cunningham ML, 2006 Modes of action and species-specific effects of di-(2-ethylhexyl)phthalate in the liver. Crit. Rev. Toxicol. 36 (5), 459–479. doi:10.1080/10408440600779065. [PubMed: 16954067]

Samaraweera M, Jolin W, Vasudevan D, MacKay AA, Gascón JA, 2014 Atomistic prediction of sorption free energies of cationic aromatic amines on Montmorillonite: a linear interaction energy method. Environ. Sci. Technol. Lett. 1 (6), 284–289. doi:10.1021/ez500136g.

Shankar A, Teppala S, 2011 Relationship between urinary bisphenol A levels and diabetes mellitus. J. Clin. Endocrinol. Metab. 96 (12), 3822–3826. doi:10.1210/jc.2011-1682. [PubMed: 21956417]

Shockey WA, Kieslich CA, Wilder CL, Watson V, Platt MO, 2019 Dynamic model of protease state and inhibitor trafficking to predict protease activity in breast cancer cells. Cell. Mol. Bioeng. 12 (4), 275–288. doi:10.1007/s12195-019-00580-5. [PubMed: 31719914]

Song JH, Murphy RJ, Narayan R, Davies GBH, 2009 Biodegradable and compostable alternatives to conventional plastics. Phil. Trans. R. Soc. B 364, 2127–2139. doi:10.1098/rstb.2008.0289. [PubMed: 19528060]

Sposito G, Skipper NT, Sutton R, Park S. h., Soper AK, 1999 Greathouse, J. A. Surface geochemistry of the clay minerals.. Proc. Natl. Acad. Sci. 96, 3358–3364. doi:10.1073/pnas.96.7.3358. [PubMed: 10097044]

Sterling T, Irwin JJ, 2015 ZINC 15–Ligand discovery for everyone. J. Chem. Inf. Model. 55, 2324–2337. doi:10.1021/acs.jcim.5b00559. [PubMed: 26479676]

Swan SH, et al., 2005 . Decrease in anogenital distance among male infants with prenatal phthalate exposure. Environ. Health Perspect. 113 (8), 1056–1061. doi:10.1289/ehp.8100. [PubMed: 16079079]

Talsness CE, Andrade AJM, Kuriyama SN, Taylor JA, vom Saal FS, 2009 Components of plastic: experimental studies in animals and relevance for human health. Philos. Trans. R. Soc.Lond. Ser. B, Biol. Sci. 364 (1526), 2079–2096. doi:10.1098/rstb.2008.0281. [PubMed: 19528057]

Tamamis P, Adler-Abramovich L, Reches M, Marshall K, Sikorski P, Serpell L, Gazit E, Archontis G, 2009 Self-assembly of phenylalanine oligopeptides: insights from experiments and simulations. Biophys. J. 96 (12), 5020–5029. doi:10.1016/j.bpj.2009.03.026. [PubMed: 19527662]

Tamamis P, Kasotakis E, Mitraki A, Archontis G, 2009 Amyloid-like self-assembly of peptide sequences from the adenovirus fiber shaft: insights from molecular dynamics simulations. J. Phys. Chem. B 113 (47), 15639–15647. doi:10.1021/jp9066718. [PubMed: 19863125]

Tamamis P, Kasotakis E, Archontis G, Mitraki A, 2014 Combination of theoretical and experimental approaches for the design and study of fibril-forming peptides. Methods Mol. Biol. 1216, 53–70. doi:10.1007/978-1-4939-1486-9_3. [PubMed: 25213410]

Tao K, Chen Y, Orr AA, Tian Z, Makam P, Gilead S, Si MS, Rencus-Lazar S, Qu SN, Zhang MJ, Tamamis P, Gazit E, 2020 Enhanced fluorescence for bioassembly by environment-switching doping of metal ions. Adv. Funct. Mater. 30, 1909614. doi:10.1002/adfm.201909614. [PubMed: 32256278]

Tarapore P, Ying J, Ouyang B, Burke B, Bracken B, Ho SM, 2014 Exposure to bisphenol A correlates with early-onset prostate cancer and promotes centrosome amplification and anchorage-independent growth in vitro. PLoS One 9 (3). doi:10.1371/journal.pone.0090332, e90332. [PubMed: 24594937]

Teuten EL, Saquing JM, Knappe DRU, Barlaz MA, Jonsson S, Björn A, Rowland SJ, Thompson RC, Galloway TS, Yamashita R, et al., 2009 . Transport and release of chemicals from plastics to the environment and to wildlife. Philos. Trans. R. Soc. B Biol. Sci. 364, 2027–2045. doi:10.1098/rstb.2008.0284.

Toor R, Mohseni M, 2007 UV-H2O2 based AOP and its integration with biological activated carbon treatment for DBP reduction in drinking water. Chemosphere 66 (11), 2087–2095. doi:10.1016/j.chemosphere.2006.09.043. [PubMed: 17095044]

Tsai W-T, Lai C-W, Su T-Y, 2006 Adsorption of bisphenol-A from aqueous solution onto minerals and carbon adsorbents. J. Haz. Mat. 134 (1–3), 169–175. doi:10.1016/j.jhazmat.2005.10.055.

Ullah H, Jahan S, Ain QU, Shaheen G, Ahsan N, 2016 Effect of bisphenol S exposure on male reproductive system of rats: a histological and biochemical study. Chemosphere 152, 383–391. doi:10.1016/j.chemosphere.2016.02.125. [PubMed: 26994432]

Ullah A, Pirzada M, Jahan S, Ullah H, Khan MJ, 2019 Bisphenol A analogues bisphenol B, bisphenol F, and bisphenol S induce oxidative stress, disrupt daily sperm production, and damage DNA in rat spermatozoa: a comparative in vitro and in vivo study. Toxicol. Ind. Health 35 (4), 294–303. doi:10.1177/0748233719831528. [PubMed: 30871434]

Vanommeslaeghe K, MacKerell AD, 2012 Automation of the charmm general force field (CGenFF) I: bond perception and atom typing. J. Chem. Inf. Model. 52, 3144–3154. doi:10.1021/ci300363c. [PubMed: 23146088]

Vanommeslaeghe K, Hatcher E, Acharya C, Kundu S, Zhong S, Shim J, Mackerell AD, 2010 CHARMM general force field: a force field for drug-like molecules compatible with the CHARMM all-atom additive biological force fields. J. Comput. Chem. 31 (4), 671–690. doi:10.1002/jcc.21367. [PubMed: 19575467]

Vanommeslaeghe K, Raman EP, MacKerell AD, 2012 Automation of the CHARMM General Force Field (CGenFF) II: assignment of bonded parameters and partial atomic charges. J. Chem. Inf. Model. 52 (12), 3155–3168. doi:10.1021/ci3003649. [PubMed: 23145473]

Viñas P, Campillo N, Martínez-Castillo N, Hernández-Córdoba M, 2010 Comparison of two derivatization-based methods for solid-phase microextraction-gas chromatography-mass spectrometric determination of bisphenol A, bisphenol S and biphenol migrated from food cans. Anal. Bioanal. Chem. 397 (1), 115–125. doi:10.1007/s00216-010-3464-7. [PubMed: 20127078]

Wang F, Landau DP, 2001 Efficient, multiple-range random walk algorithm to calculate the density of states. Phys. Rev. Lett. 86 (10), 2050–2053. doi:10.1103/PhysRevLett.86.2050. [PubMed: 11289852]

Wang M, Phillips TD, 2019 Potential applications of clay-based therapy for the reduction of pesticide exposures in humans and animals. Appl. Sci. 9, 5325. doi:10.3390/app9245325. [PubMed: 32944385]

Wang T, Li M, Chen B, Xu M, Xu Y, Huang Y, Lu J, Chen Y, Wang W, Li X, Liu Y, Bi Y, Lai S, Ning G, 2012 Urinary bisphenol A (BPA) concentration associates with obesity and insulin resistance. J. Clin. Endocrinol. Metab. 97 (2). doi:10.1210/jc.2011-1989, E223–E227. [PubMed: 22090277]

Wang Y, Gkeka P, Fuchs JE, Liedl KR, Cournia Z, 2016 DPPC-cholesterol phase diagram using coarse-grained molecular dynamics simulations. Biochim. Biophys. Acta. 1858 (11), 2846–2857. doi:10.1016/j.bbamem.2016.08.005. [PubMed: 27526680]

Wang M, Maki CR, Deng Y, Tian Y, Phillips TD, 2017 Development of High Capacity Enterosorbents for Aflatoxin B1 and Other Hazardous Chemicals. Chem. Res. Toxicol. 30 (9), 1694–1701. doi:10.1021/acs.chemrestox.7b00154. [PubMed: 28768106]

Wang Y, Latshaw DC, Hall CK, 2017 Aggregation of Aβ(17–36) in the presence of naturally occurring phenolic inhibitors using coarse-grained simulations. J. Mol. Biol. 429 (24), 3893–3908. doi:10.1016/j.jmb.2017.10.006, 2017. [PubMed: 29031698]

Wang M, Orr AA, He S, Dalaijamts C, Chiu WA, Tamamis P, Phillips TD, 2019 Montmorillonites can tightly bind glyphosate and paraquat reducing toxin exposures and toxicity. ACS Omega 4, 17702–17713. doi:10.1021/acsomega.9b02051. [PubMed: 31681876]

Wang M, Hearon SE, Johnson NM, Phillips TD, 2019 Development of broad-acting clays for the tight adsorption of benzo[a]pyrene and aldicarb. Appl. Clay Sci., Appl. Clay Sci. 168, 196–202. doi:10.1016/j.clay.2018.11.010. [PubMed: 31435120]

Willemsen JAR, Myneni SCB, Bourg IC, 2019 Molecular dynamics simulations of the adsorption of phthalate esters on smectite clay surfaces. J. Phys. Chem. C 123 (22), 13624–13636. doi:10.1021/acs.jpcc.9b01864.

Wilson NK, Chuang JC, Morgan MK, Lordo RA, Sheldon LS, 2007 An observational study of the potential exposures of preschool children to pentachlorophenol, bisphenol-A, and nonylphenol at home and daycare. Environ. Res. 103, 9–20. doi:10.1016/j.envres.2006.04.006. [PubMed: 16750524]

Wirasnita R, Mori K, Toyama T, 2018 Effect of activated carbon on removal of four phenolic endocrine-disrupting compounds, bisphenol A, bisphenol F, bisphenol S, and 4-tert-butylphenol in constructed wetlands. Chemosphere 210, 717–725. doi:10.1016/j.chemosphere.2018.07.060. [PubMed: 30036819]

Xu H, Shao X, Zhang Z, Zou Y, Wu X, Yang L, 2013 Oxidative stress and immune related gene expression following exposure to di-n-butyl phthalate and diethyl phthalate in zebrafish embryos. Ecotoxicol. Environ. Saf. 93, 39–44. doi:10.1016/j.ecoenv.2013.03.038. [PubMed: 23676468]

Zerze GH, Stillinger FH, Debenedetti PG, 2020 Computational investigation of retro-isomer equilibrium structures: intrinsically disordered, foldable, and cyclic peptides. FEBS Lett. 594 (1), 104–113. doi:10.1002/1873-3468.13558. [PubMed: 31356683]

Zhang MH, Dong H, Zhao L, Wang DX, Meng D, 2019 A review on Fenton process for organic wastewater treatment based on optimization perspective. Sci. Total Environ. 670, 110–121. doi:10.1016/j.scitotenv.2019.03.180. [PubMed: 30903886]

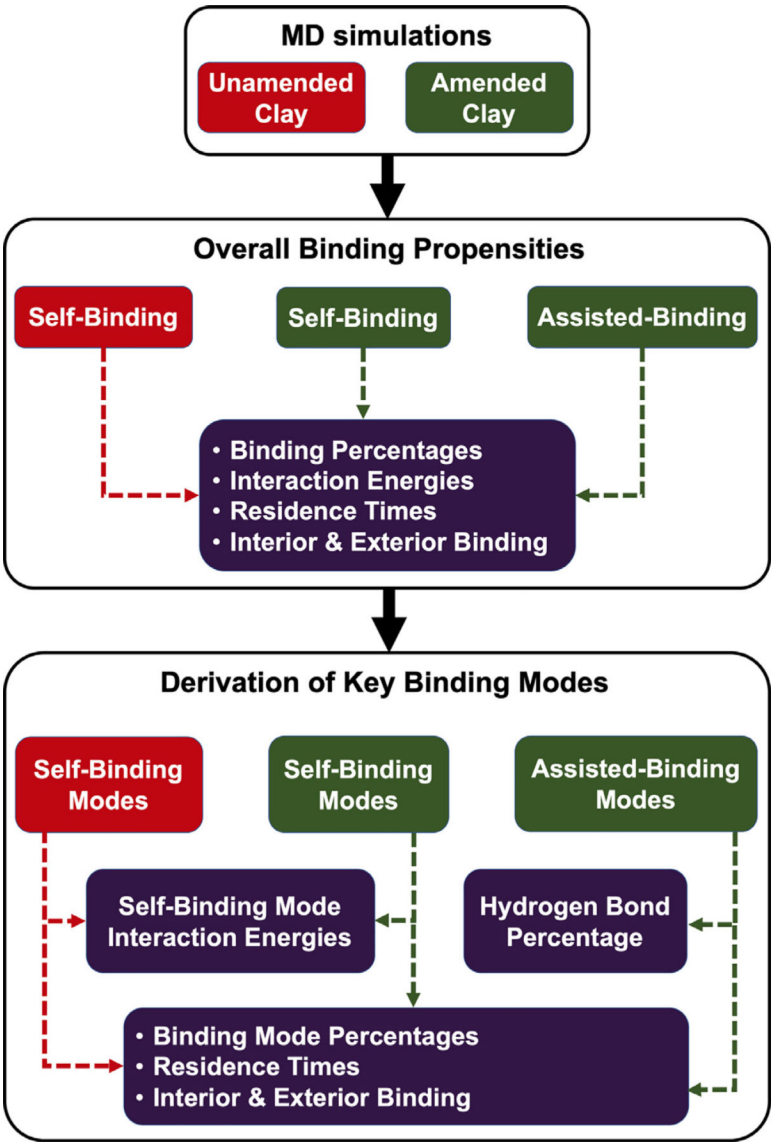

Fig. 1.

Overview of the computational analysis procedure used to investigate the binding of toxic compounds with unamended or amended clay. Red labels and arrows indicate analysis performed for the unamended clay. Green labels and arrows indicate analysis performed for the amended clay. (For interpretation of the references to color in this figure legend, the reader is referred to the web version of this article.).

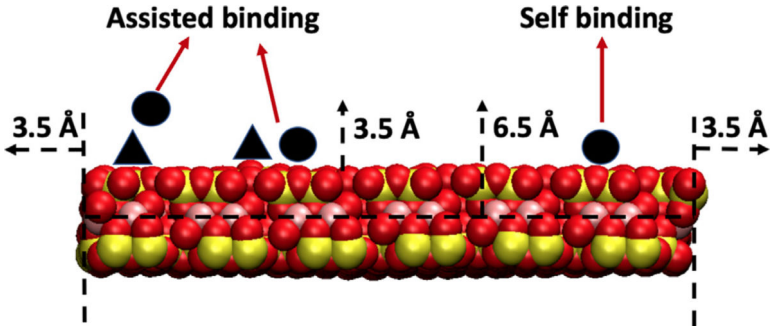

Fig. 2.

Schematic of the geometric criteria and definitions for self-binding and assisted-binding. Circles represent toxic compounds and triangles represent amending compounds. A compound with at least one atom within a distance cutoff of 3.5 Å from the clay was considered to be binding to the clay.

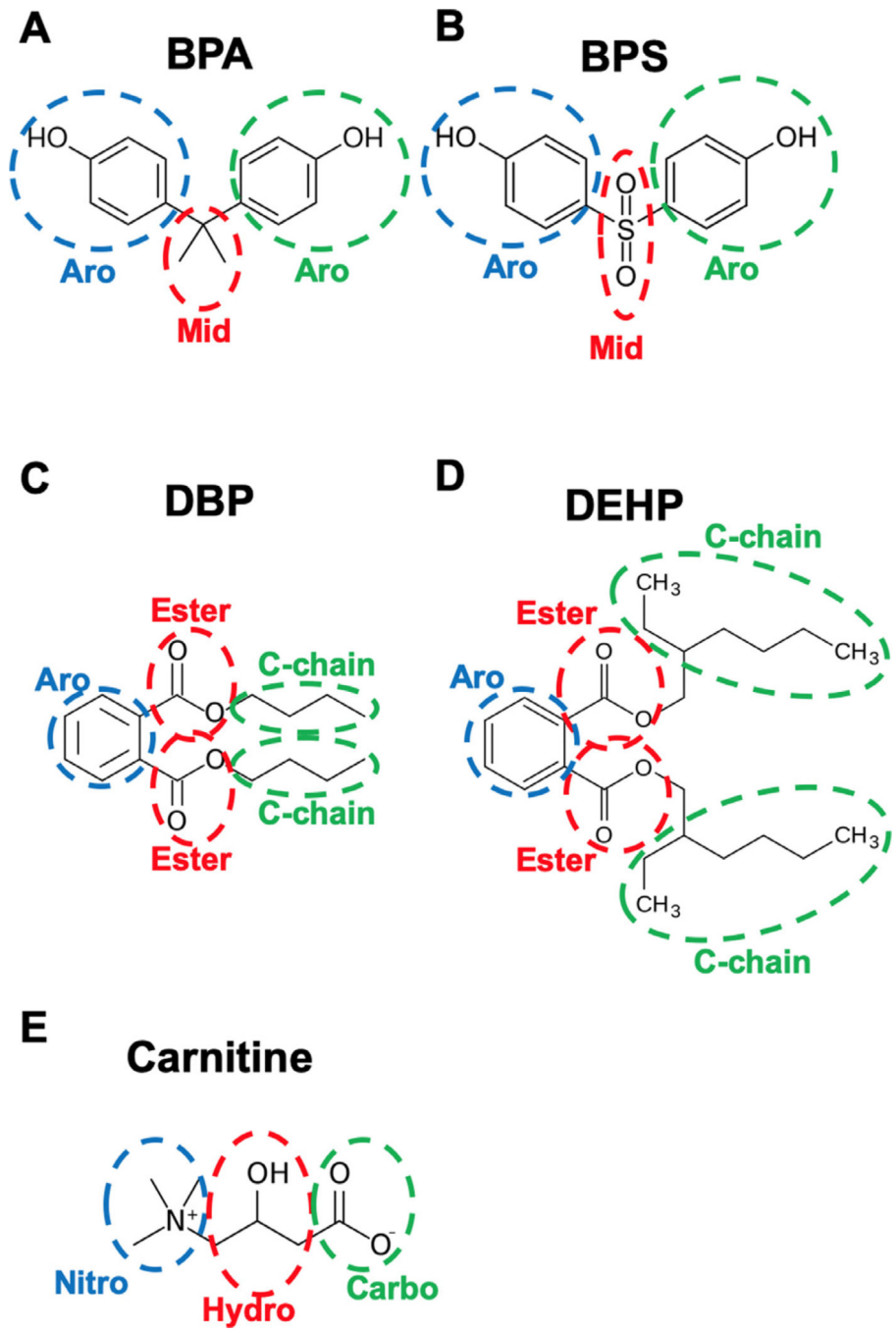

Fig. 3.

Functional groups for (A) BPA, (B) BPS, (C) DBP, (D) DEHP, and (E) carnitine defined based on geometry and chemical groups.

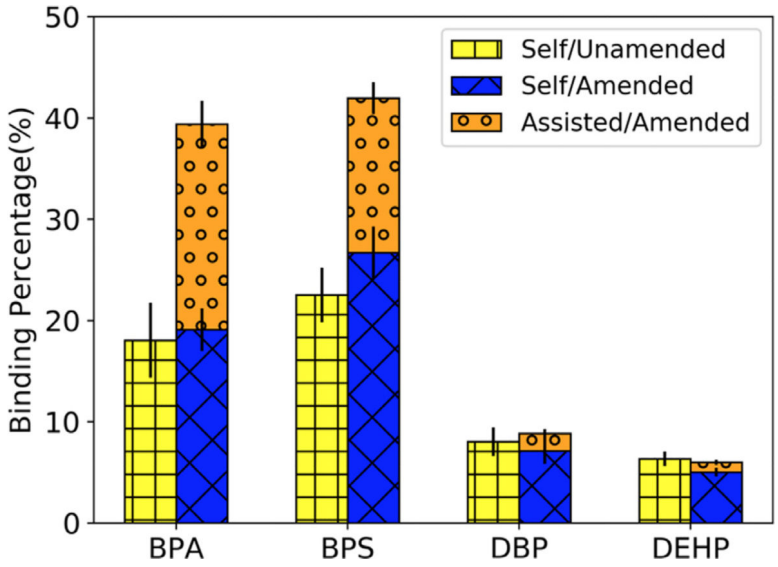

Fig. 4.

Overall binding percentages of BPA, BPS, DBP, and DEHP. “Self/Unamended” (colored yellow with “+” pattern) corresponds to self-binding to unamended clay, “Self/Amended” (colored blue with “x” pattern) corresponds to self-binding to amended clay, and “Assisted/Amended” (colored orange with “o” pattern) corresponds to assisted-binding to amended clay. Reported binding percentage values and error bars correspond to the average binding percentage across the quintet simulations and the standard error, respectively. (For interpretation of the references to color in this figure legend, the reader is referred to the web version of this article.).

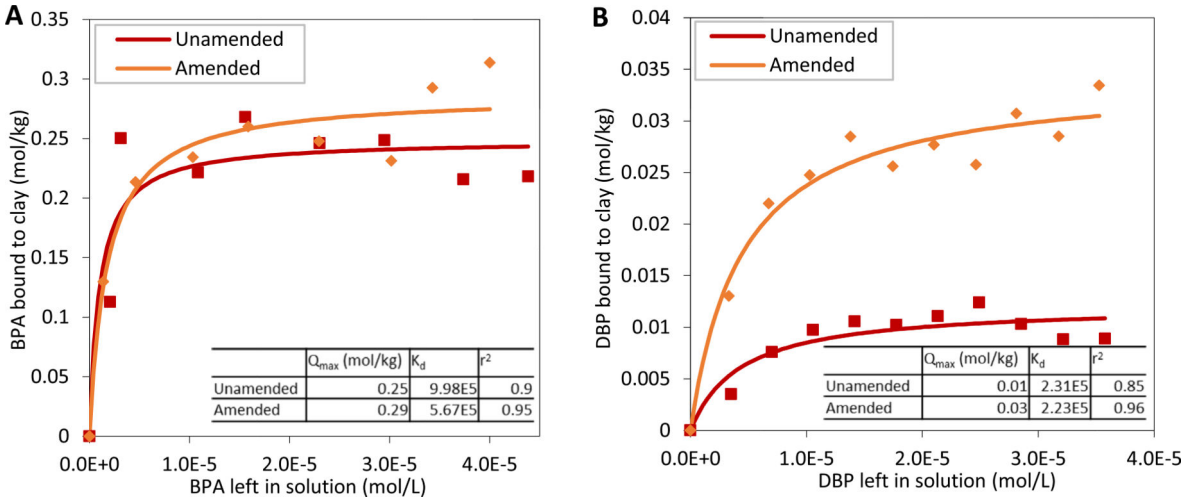

Fig. 5.

Isothermal data (diamonds and squares) and Langmuir plots (curves) of (A) BPA and (B) DBP binding onto unamended and amended clays.

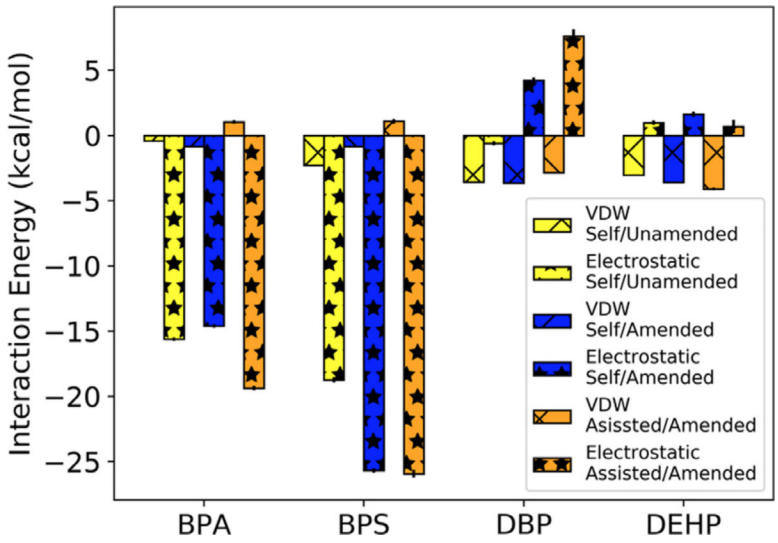

Fig. 6.

Average interaction energies decomposed into van der Waals (“x” pattern) and electrostatic (“*” pattern) components for self-binding and assisted-binding of BPA, BPS, DBP, and DEHP. “Self/Unamended” (colored yellow) corresponds to self-binding to unamended clay, “Self/Amended” (colored blue) corresponds to self-binding to amended clay, and “Assisted/Amended” (colored orange) corresponds to assisted-binding to amended clay. (For interpretation of the references to color in this figure legend, the reader is referred to the web version of this article.).

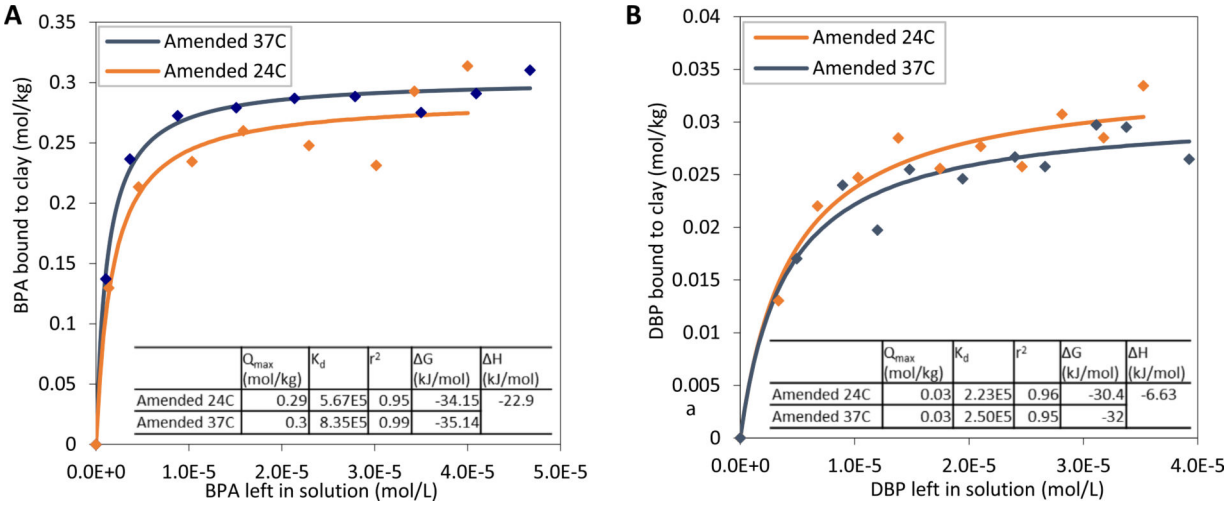

	Q_{max} (mol/kg)	K_d	r^2	ΔG (kJ/mol)	ΔH (kJ/mol)
Amended 24C	0.29	5.67E5	0.95	-34.15	-22.9
Amended 37C	0.3	8.35E5	0.99	-35.14	

a

	Q_{max} (mol/kg)	K_d	r^2	ΔG (kJ/mol)	ΔH (kJ/mol)
Amended 24C	0.03	2.23E5	0.96	-30.4	-6.63
Amended 37C	0.03	2.50E5	0.95	-32	

Fig. 7.

Isothermal data (diamonds) and Langmuir plots (curves) of (A) BPA and (B) DBP binding onto amended clays at two temperatures.

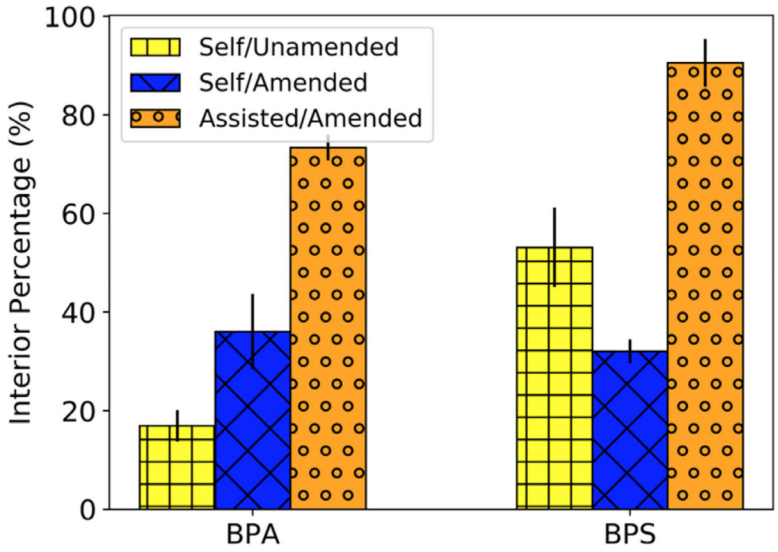

Fig. 8.

Percentages of BPA/BPS binding to the interior of the clay given a binding instance. “Self/Unamended” corresponds to self-binding to unamended clay (colored yellow with “+” pattern), “Self/Amended” corresponds to self-binding to amended clay (colored blue with “x” pattern), and “Assisted/Amended” corresponds to assisted-binding to amended clay (colored orange with “o” pattern). Error bars are one standard error. (For interpretation of the references to color in this figure legend, the reader is referred to the web version of this article.).

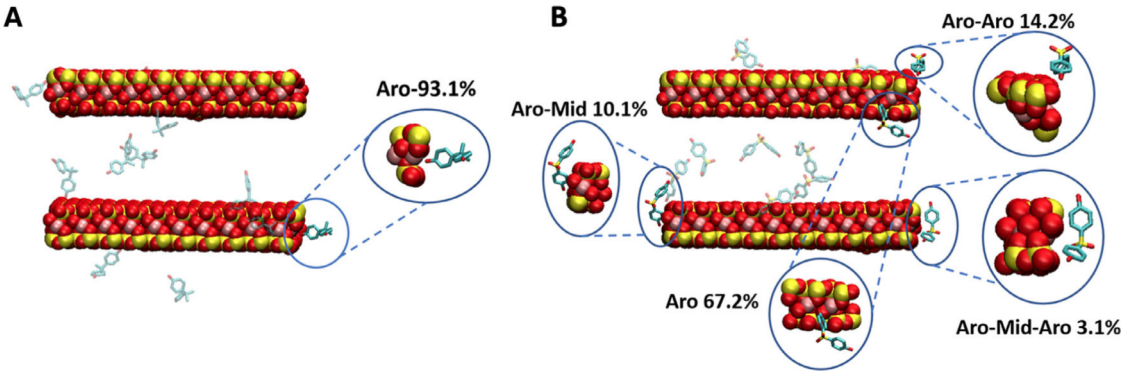

Fig. 9.

Molecular graphics images of the predominant self-binding modes of (A) BPA and (B) BPS with unamended clay and their corresponding percentages. Zoomed in molecular graphics images of the predominant self-binding modes of (A) BPA and (B) BPS with unamended clay are encircled in blue.

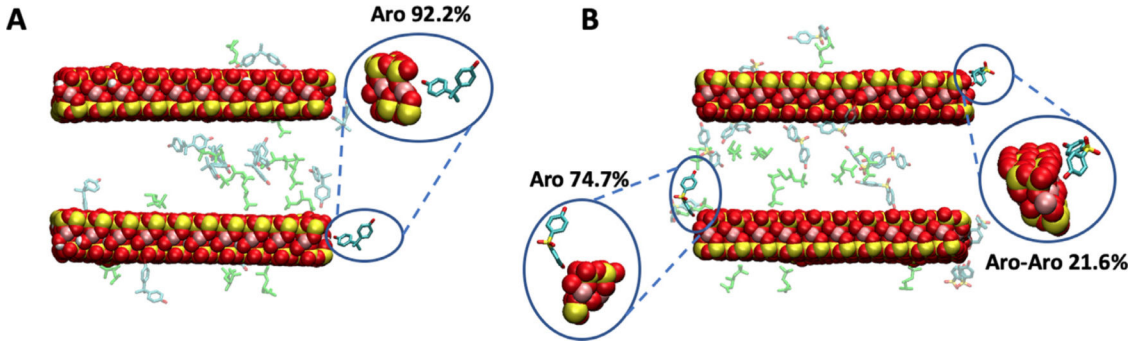

Fig. 10.

Molecular graphics images of the predominant self-binding modes of (A) BPA and (B) BPS with amended clay and their corresponding percentages. The amending compound, carnitine. is colored green. Zoomed in molecular graphics images of the predominant self-binding modes of (A) BPA and (B) BPS with amended clay are encircled in blue. (For interpretation of the references to color in this figure legend, the reader is referred to the web version of this article.).

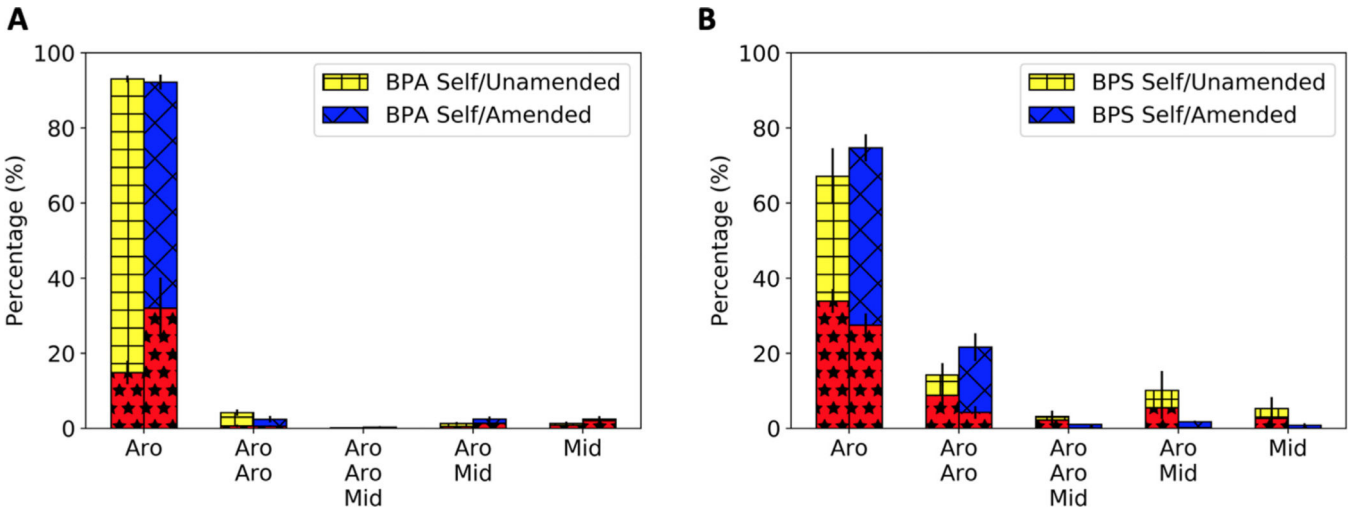

Fig. 11.

Percentages of (A) BPA and (B) BPS self-binding modes with unamended and amended clays and their respective interior binding percentages. Red portion of every bar with pattern "*" is the percentage of the given self-binding mode within the interior of the clay. "Self/Unamended" corresponds to self-binding to unamended clay (colored yellow with "+" pattern), and "Self/Amended" corresponds to self-binding to amended clay (colored blue with "x" pattern). (For interpretation of the references to color in this figure legend, the reader is referred to the web version of this article.).

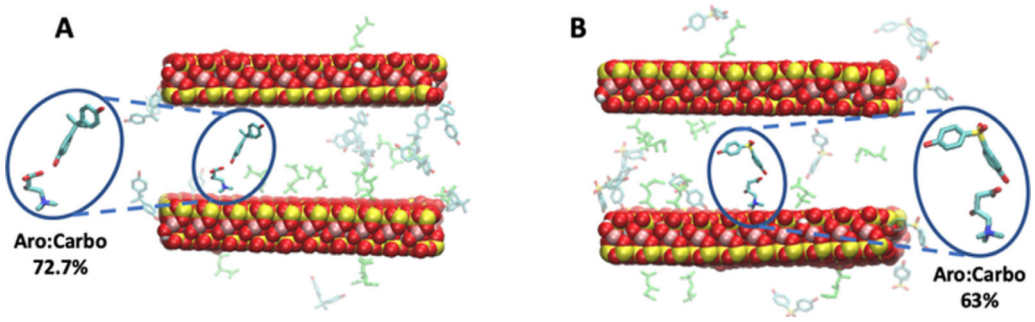

Fig. 12.

Molecular graphics images of the predominant assisted-binding mode of (A) BPA and (B) BPS with amended clay and their corresponding percentages. The amending compound, carnitine. is colored green. Zoomed in molecular graphics images of the assisted-binding mode of (A) BPA and (B) BPS with amended clay are encircled in blue. (For interpretation of the references to color in this figure legend, the reader is referred to the web version of this article.).

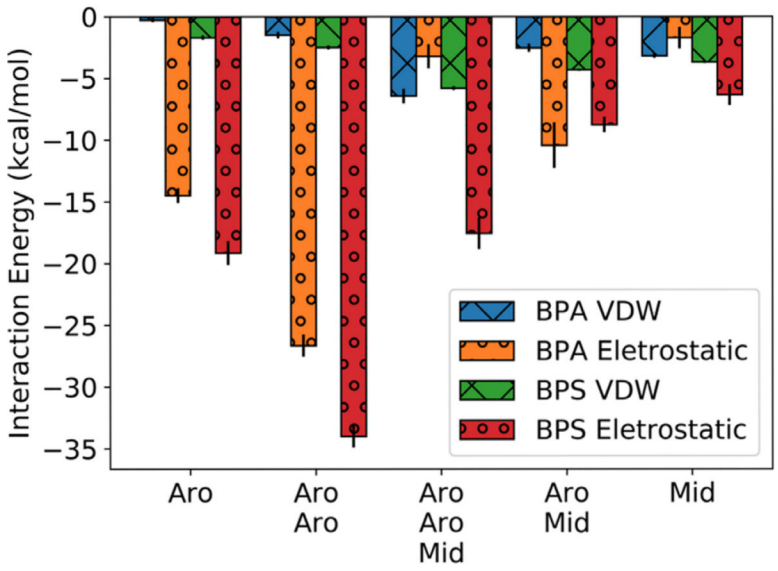

Fig. 13.

Interaction energies of individual BPA and BPS self-binding modes with unamended clay decomposed into van der Waals (VDW, “x” pattern) and electrostatic (“o” pattern) components. The van der Waals component for BPA and BPS self-binding modes are colored blue and green, respectively. The electrostatic component for BPA and BPS self-binding modes are colored orange and red, respectively. Error bars are one standard error. (For interpretation of the references to color in this figure legend, the reader is referred to the web version of this article.).